



UPPSALA  
UNIVERSITET

UPTEC K 25001

Examensarbete 30 hp

Januari 2025

# Computational Investigation of Oxidative Addition Step in Palladium-catalyzed Reactions

---

Wijitchakhorn, Watthachak



UPPSALA  
UNIVERSITET

## Computational Investigation of Oxidative Addition Step in Palladium-catalyzed Reactions

---

Wijitchakhorn, Watthachak

### Abstract

Palladium-catalyzed cross-coupling reactions, for instance Suzuki-Miyaura (SM), Heck and Sonogashira reactions, are essential in synthetic organic chemistry for forming carbon-carbon bonds. These reactions play a critical role in pharmaceutical development, enabling the synthesis of complex molecules used to treat medical conditions.

This thesis focuses on the oxidative addition (OA) step, one of the pivotal stages in the catalytic cycle of cross-coupling reactions, where palladium coordinates with aryl halides to initiate bond formation. Using density functional theory (DFT) calculations, the study investigates the steric effects of various monodentate phosphine ligands and aryl halide substrates on the reactivity and selectivity of oxidative addition. Transition state modelling was employed to determine energy barriers and mechanistic pathways, providing insights into ligand and substrate reactivity.

Key findings reveal that while the steric effects of the ligand were shown to affect the reactivity of OA by increasing the energy barrier, it was not conclusive that the change in reactivity is due to steric effects alone, suggesting other factors in play. Meanwhile, the substrate's steric effects were shown to decrease energy barrier, which increases the reactivity of OA reaction. Additionally, it was shown that substrates with steric bulk capable of interfering with coordination sites also enhanced reactivity. As it seems, the steric effect was not enough to explain the results, requiring further inspection into the other properties of the substrates and ligand, for instance the electronic properties, multiple coordinated ligands and the effects of substituents of aryl halides.

Teknisk-naturvetenskapliga fakulteten

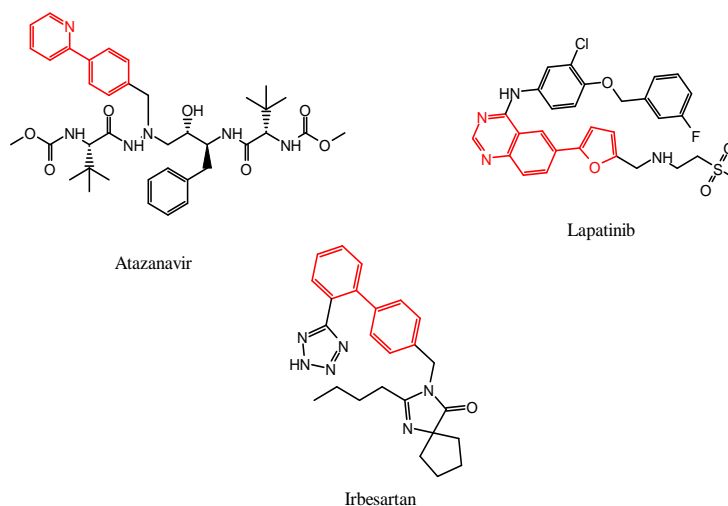
Uppsala universitet, Utgivningsort Uppsala/Visby

Handledare: Christian Sköld Ämnesgranskare: Henning Henschel

Examinator: Christian Sköld

# Populärvetenskaplig sammanfattning

I dagens forskning om katalytiska reaktioner spelar förståelsen för hur molekyler interagerar och reagerar en central roll. Denna studie använder avancerade datorsimuleringar för att undersöka de grundläggande mekanismerna bakom oxidativ addition, en nyckelreaktion i palladiumkatalyserade korskopplingsreaktioner. Korskopplingsreaktioner är oumbärliga inom läkemedelsforskning och materialvetenskap, då de möjliggör bildandet av kol-kol-bindningar, en viktig byggsten för många kemiska föreningar. Många av kommersiella läkemedel ute på marknaden är beroende av korskoppling reaktioner, som exempelvis bromsmedicinet mot HIV atazanavir, bröstcancerbehandling lapatinib och blodtryckssänkande irbesartan, som visas nedan, där rödmarkerade fragment är produkten av korskopplingsreaktion.



Genom att simulera reaktionsförloppet kan vi förstå hur olika faktorer, såsom liganders och substratets strukturer, påverkar reaktiviteten och selektiviteten i dessa reaktioner. Speciellt fokuserar studien på hur steriska hinder hos fosfinligander och arylhalider styr reaktionsförloppet. Genom att undersöka dessa aspekter kan vi inte bara förutse reaktionens hastighet utan även prediktera produkten, vilket öppnar möjligheter för att utveckla reaktioner för specifika behov.

Beräkningsstudier erbjuder flera fördelar jämfört med experimentella metoder. De gör det möjligt att analysera reaktioner som kan vara svåra eller dyra att utföra i laboratoriet. Med hjälp av simuleringar kan olika hypoteser testas och en syntesplan kan optimeras utan att använda stora mängder material eller kemikalier. Dessutom ger de detaljerad information om övergångstillstånd och energibarriärer, vilket ger insikter som inte alltid är tillgängliga genom experimentella tekniker. Denna kombination av precision och kostnadseffektivitet gör datorsimuleringar till ett kraftfullt verktyg för modern katalysforskning.

## Abbreviations

---

B3LYP	Becke, 3-parameter, Lee-Yang-Parr functional
BJ	Becke-Johnson damping
D3	Grimme's dispersion correction
DFT	Density functional theory
et al.	et alia
HOMO	Highest Occupied Molecular Orbital
LACV3P*	Los Alamos double zeta basis set with polarization
LUMO	Lowest Unoccupied Molecular Orbital
OA	Oxidative addition
PBE0	Perdew-Burke-Ernzerhof functional
SM	Suzuki-Miyaura
S <sub>N</sub> 2	Bimolecular nucleophilic substitution
THF	Tetrahydrofuran
TS	Transition state

# Table of Contents

---

1	Introduction .....	1
1.1	Palladium-catalyzed cross coupling reactions .....	1
1.1.1	Oxidative addition .....	2
1.2	Previous studies .....	3
1.3	Aims .....	5
2	Computational methods .....	6
3	Results and discussion .....	7
3.1	Phosphine ligands and aryl halide substrates.....	7
3.2	Computational modeling of transition states and energy barriers.....	9
3.3	Free energy profile of the transition states .....	10
3.3.1	Ligand's steric effects .....	11
3.3.2	Substrate's steric effects.....	14
4	Conclusion.....	19
	Acknowledgements .....	20
	References .....	21
	Appendices .....	24

# 1 Introduction

---

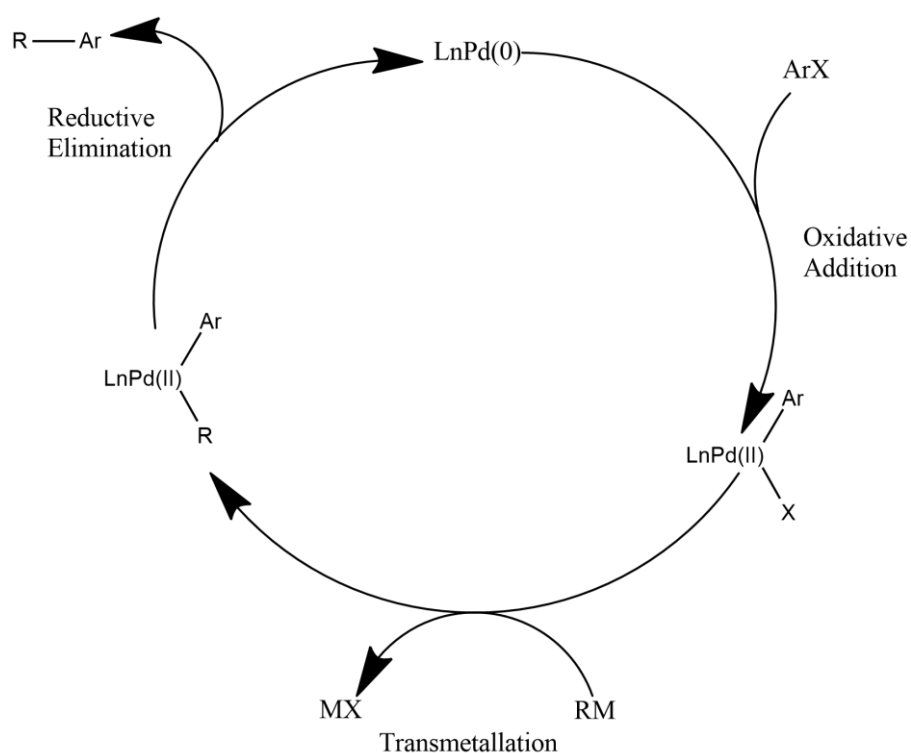
In the field of medicinal chemistry, there are considerations to be made when designing and synthesizing a compound as there are many ways to navigate the synthetic route. What reactions to employ to enable the most straightforward synthesis and, with the chosen reaction, what reagents are safe, readily available, economically and environmentally friendly? Medicinal chemists answer these questions and often reach similar conclusions as certain reactions such as amide bond formation and Suzuki-Miyaura (SM) coupling are shown to be some of the commonly employed reactions in medicinal chemistry [1]. SM cross-coupling has shown a tremendous increase in use due to the possibility of carbon-carbon bond formation, the rise of new reagents and development of new ligands for the metal catalysts which primarily consist of palladium-, nickel- and copper metal. Palladium-catalyzed cross-coupling reactions have since enabled synthesis of various compounds in drug discovery targeting medical conditions such as migraine, hypertension, cystic fibrosis and many more [2].

## 1.1 Palladium-catalyzed cross coupling reactions

Palladium-catalyzed cross-coupling reaction is, as mentioned, a powerful tool for medicinal chemists to synthesize their target molecule. Cross-coupling reactions have three important components to be considered, those are the substrate, the metal catalyst and the ligand. As for the catalysts, there are many catalysts which have been used in various cross-coupling reactions, one of which is palladium catalyst, specifically the highly reactive palladium(0) catalyst [3]. The metal catalyst is used to facilitate the C-C bond formation by coordinating the substrates and subsequent exchanging and releasing of molecular fragments. Performance of the metal catalyst is affected by the ligands coordinating with the metal atom which are used to facilitate stability, reactivity and selectivity of the metal catalyst. For palladium, one large class of ligands is phosphine ligands due to their ability to form strong bond to metal catalyst and the ease of electronic and steric properties tuning by changing substituents [4]. Additionally, many phosphine ligands are available as chiral ligands which can produce stereoselective reaction outcomes, for example in the synthesis of atropisomers via SM reactions [5].

Mechanistically, palladium-catalyzed cross-coupling reaction commonly consists of 3 key reaction steps, oxidative addition, transmetalation and reductive elimination. For instance, Scheme 1 shows the mechanism of SM cross-coupling reaction as a catalytic cycle starting with oxidative addition which involves the palladium catalyst forming a bond with the halide and the organic substrate. This increases the oxidation state of the palladium center from Pd(0) to +2. Following this, in the transmetalation step, the organic group from the palladium complex is exchanged with another organic moiety. And finally, in the reductive elimination step, the two organic groups are coupled together, results in the formation of C-C bond and the palladium catalyst is reduced from oxidation state +2 back to its active oxidation state Pd(0).

**Scheme 1.** Catalytic cycle of SM cross-coupling reaction with Pd catalyst

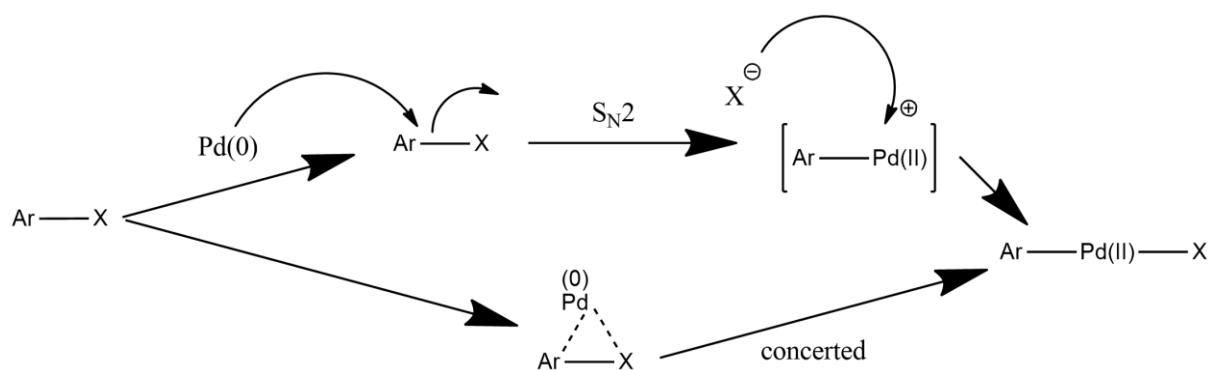


### 1.1.1 Oxidative addition

Oxidative addition (OA) is a common first step in the catalytic cycle of cross-coupling reactions with Pd catalysts, where the metal complex coordinates with the halide and the carbon, this increases the oxidation state of the metal by +2 [6]. For reactions where OA is the first step of cross-coupling reactions, investigation of this step will elucidate the mechanism of action between the interacting organic halide and the metal catalyst. There are many mechanistic pathways for OA, some of which are concerted mechanism (three-centered),  $\text{S}_{\text{N}}2$ -mechanism and radical mechanism. Previous computational studies [6-9] suggest that the concerted mechanism and the  $\text{S}_{\text{N}}2$ -mechanism dominate in cross-coupling reactions, providing a more predictable pathway for oxidative addition. In contrast, the radical mechanism remains less thoroughly mapped, with its occurrence being highly sensitive to subtle changes reaction conditions [10].

Concerted mechanism and  $\text{S}_{\text{N}}2$ -mechanism in OA differ in the geometric features. For  $\text{S}_{\text{N}}2$ -mechanism, the nucleophile (Pd-complex) approaches the electrophilic center (aryl halide) through the aromatic ring, this leaves no interaction between Pd and the halide. Whereas for concerted mechanism, the Pd interacts simultaneously with the substrate (aryl group) and the leaving group (halide), forming a three-centered transition state with trigonal planar geometry. Regardless of the mechanism, the product formed will result in square planar geometry [6].

**Scheme 2.** Common oxidative addition mechanisms



To steer which mechanism will occur, this can be done by varying substrate, and ligand [9]. This can be controlled by understanding ligand electronic and steric properties, nature of the aryl halide substrate, and coordination number of Pd-catalyst complex. Firstly, the ligand's properties dictate the bite angle of the complex based on its steric properties, namely its steric bulk and spatial arrangement. With monoligated complex, there is less steric hindrance compared to a bidentate complex. This results in the monoligated complex having the larger bite angle and resulting in a flexible, spatial arrangement which facilitates the crowded concerted mechanism. Secondly, the leaving group can decide the mechanistic pathway, for halides (F, Cl, Br and I), the concerted mechanism is favorable as this allows interaction between the Pd and the leaving group, favoring three-centered geometry.

Besides the leaving group, the major contribution stems from the nature of Pd-complex. The geometry of the Pd-complex changes based on the number of coordinated ligands, which affects how it interacts with the substrate due to the differing shape of molecular orbitals between a monoligated and bidentate complex. In monoligated complexes, the spatial orientation of the Pd-center molecular orbitals enables effective overlap with both the aryl carbon and the leaving group, promoting interactions between Pd atom and C-X atoms, which can facilitate concerted mechanism. Whereas for bidentate complexes, the shape of molecular orbital enables effective interaction with the aryl carbon, leaving no interaction between Pd and leaving group, resembling  $S_N2$ -mechanism. Therefore, to induce concerted mechanism for the model system using aryl halide and Pd metal complex, monoligated complex is preferred [9].

## 1.2 Previous studies

Oxidative addition of aryl halides (Ar-X) into Pd(0) complexes has attracted significant attention in experimental and theoretical research due to its extensive application in organic synthesis. Studies were conducted to investigate the reactivity of ligand or aryl halide and to identify the leading property which affects reactivity of OA.

Norrby et al. [11][12] investigated monoligated 12-electron Pd-complex or PdL as the active form of the catalyst during OA. PdL catalyst is formed from the more stable PdL<sub>2</sub> which dissociated one of the ligands to form the more reactive 12-electron complex [11]. The studies aimed to find a model system which could describe the reactivity of the aryl chlorides, which in comparison to aryl halides such as aryl bromides, are less reactive. This suggests that using the more reactive aryl bromide in this study could facilitate the identification of transition states. Additionally, the study investigated reactivity of para-substituted aryl chlorides and found that the electronic effects of the aryl chlorides substituents at para position affect reactivity, where electron deficient aryl chlorides are more reactive than the electron rich aryl chlorides [12]. The studies suggest that monoligated 12-electron Pd-complex could be implemented in a computational study involving aryl halides and its reactivity, and electronic effects of the aryl halides are of importance when investigating substrate reactivity.

Looking into the properties of ligand and aryl halide, Barder et al. [4] report the use of 2-(2',6'-dimethoxybiphenyl)-dicyclohexylphosphine (SPhos) as a ligand, which significantly enhances the reactivity of palladium complexes, even for challenging substrates like aryl chlorides and highly hindered biaryls. They compare the performance of SPhos with another ligand and investigate the role of ligand bulk and electron-donating properties. The results showed the importance of ligand design, specifically the ligand's steric and electronic effects, in improving catalyst efficiency for Suzuki-Miyaura coupling at low catalyst loadings.

However, Landeros et al. [13] have conducted an experimental study regarding ligand steric properties where they conducted a kinetic study of OA reaction using aryl halide and different ligand with varying steric bulk by increasing the steric properties of the coordinating ligand to further impose steric hindrance to the complex. The results indicated that the ligand's steric effect was not the main contributor to the change in reactivity of OA reaction.

Additionally, Jover et al. [14] did a computational study of phosphine ligand and its effects in SM cross-coupling reaction, using 4 different monophosphine ligands. While the study investigated the whole cross-coupling reaction, the study highlighted the ligand's effects on OA reaction. The study constructed a multilinear regression model which compares the ligand's electronic and steric effect through HOMO descriptor and steric descriptor. It was stated that the OA step is dictated by primarily the ligand's electronic effects and minimally on ligand steric effects.

As for the aryl halide substrate, Lu et al. [15] investigated reactivity of substrate used in OA by developing a quantitative model using molecular descriptors such as electronic, steric and bond strength descriptors. The model uses 79 aryl substrates of varying properties to highlight the key descriptors affecting OA which could be used to find an aryl halide substrate which could facilitate the reactivity of OA. Additionally, the substrates used in the model focused primarily on ortho-substituents and meta-substituents, indicating the steric effects depending on the location of the substituents in aryl halide.

Raders et al. [16] did an experimental study of sterically demanding substrates for cross-coupling reaction where they investigated the efficacy of TNpP ligand, known to show good results and yield for sterically demanding substrates. The study showed that there is a steric effect that contributes to the overall yield of cross-coupling reaction as varying the steric bulk of the substrate does result in different in isolated yield. To prove this, they investigate the OA reaction by isolating the product of OA in cross-coupling reaction. The conclusion was that there were different complexes formed during OA, where the distribution of these complexes can affect the rate of OA reactions.

Alimi et al. [17] came to a different conclusion, where they did a kinetic study of OA in nonsubstituted, ortho-substituted and meta-substituted aryl halides. The results were that the reactivity of OA decreases with ortho-substituted aryl halides as opposed to the nonsubstituted and meta-substituted substrates. However, it was emphasized that the reactivity was not affected purely by steric effects of the aryl halide, but also the electronic effects accompanying the substituents.

### **1.3 Aims**

The aim of this project is to computationally investigate oxidative addition step for palladium-catalyzed reactions to understand how different aryl halide substrates and monodentate phosphine ligands affect the reaction outcome of oxidative addition. The interactions of interest of the substrates and the ligands to be investigated will be steric hindrance and its importance on reactivity during the oxidative addition.

## 2 Computational methods

---

DFT calculations were performed with Jaguar software package [18][19] with Maestro release 2024-3 as graphical interface to calculate relative energy barriers through identifying transition state (TS). Geometry optimization and TS searches of all structures were carried out with the functional PBE0-D3(BJ) [20] with the LACV3P\* [21] basis set. Solvent effects were considered using polarizable continuum model (PCM) with THF as the solvent. For all calculated structures, vibrational frequencies analysis was conducted at the same level of theory to confirm the nature of stationary points according to the eigenvalues of the Hessian matrix. Thermodynamic properties were evaluated first with zero point energy calculation and thermal corrections were applied for  $T = 298.15$  K and  $P = 1.0$ .

The starting point structures for geometry optimization were either computationally generated or obtained from CCDC database with minor modification to fit the study's model system. Modified structures obtained from CCDC were optimized after the modification with the same level of theory as geometry optimization and TS search. Computationally generated structures were constructed through relaxed coordinate scan using the functional B3LYP-D3 and LACV3P\* basis set before further optimization. The structures shown in this work were generated from Maestro release 2024-3 interface.

## 3 Results and discussion

### 3.1 Phosphine ligands and aryl halide substrates

Choice of ligand and substrates used in the study will be crucial to shaping a good model system as both are the variables which can affect reaction outcome. In this case, different phosphine ligands and different aryl halide substrates of varying steric congestion will be computationally investigated and analysed to predict reactivity. Therefore, the substrates and phosphine ligands are selected to form a series of compounds by constructing a series of substrates and ligands with increasing steric hindrance, starting with simple substrate and ligand and ending with sterically challenging substrates and phosphine ligands as shown in Figure 1 and 2.

Some of the chosen ligands and substrates are chosen based on compounds used in previous studies as a model ligand and substrate [11][12][14], while others are chosen based on the increasing steric bulk, to fit the purpose of this study. Ligands **1** and **3** are well-known ligands used in the study of OA reaction and showed success across different substrates in theoretical studies [6][7]. Ligand **2** has been used in asymmetric reaction as a chiral ligand [22]. Similarly, ligand **4** is a commercial chiral ligand with applications in SM reaction for stereoselective synthesis [23][24]. Ligand **5** is the endpoint ligand in this investigation with similar structure as ligand **4** but bulkier and more rigid.

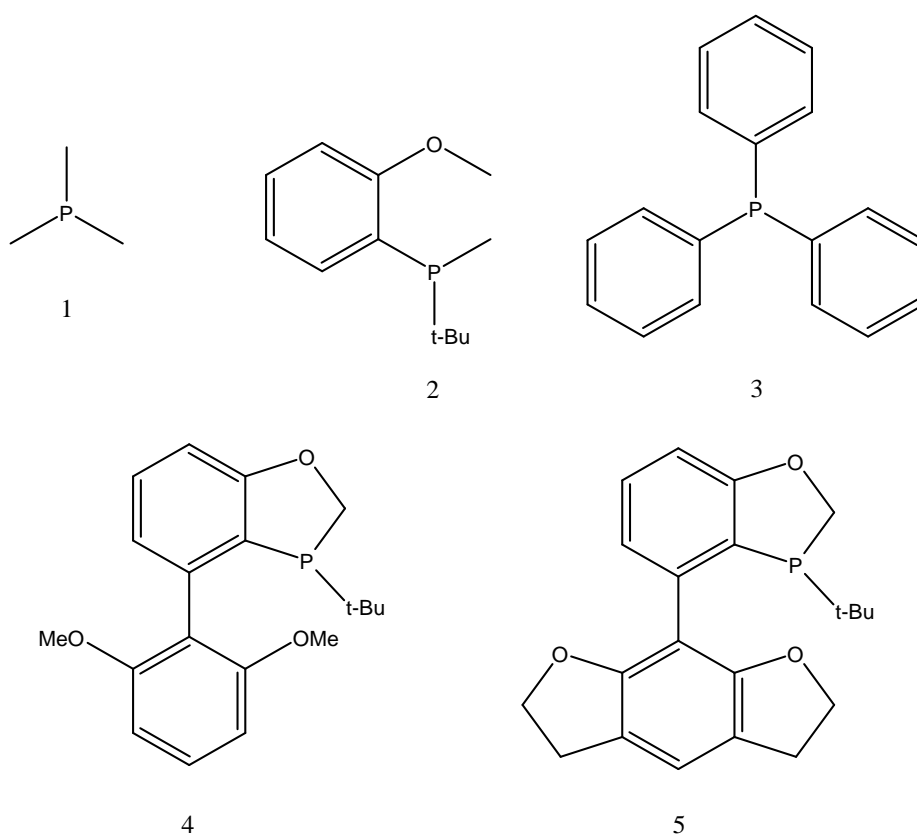


**Figure 1.** Included ligands in this study with increasing steric bulk.

As for the substrates, the choice of aryl halides is aryl bromide due to their intermediate reactivity compared to other halides. Starting simple with substrate **6** as the simplest aryl halide. Then, increasing the steric hindrance with substrates **7** and **8** which have been used in borylation reaction with similar OA reaction involved, albeit with aryl chloride counterpart which is less reactive than aryl bromide [25]. Substrates **9** and **10** are included to further provide insights into the substituent effects on reactivity and how the generated atropisomer could affect reactivity.

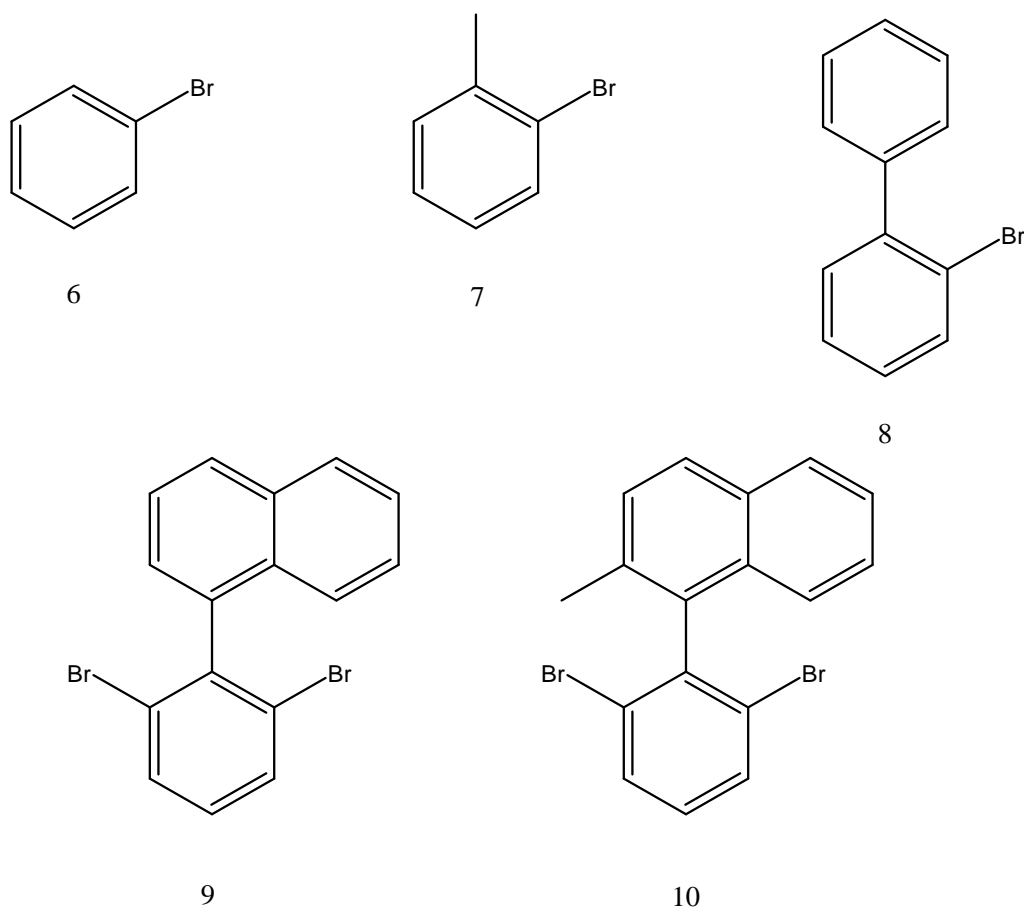


**Figure 2.** Included substrate in this study with increasing steric bulk.

### 3.2 Computational modeling of transition states and energy barriers

Transition states of substrates **6-10** with monodentate ligand **1-5** were found with the 3D structures shown in Figure B2-B26 in Appendix B, the reported values are the lowest energy structure of each complex shown in Table A2 in Appendix A. Using the optimized method as reported, most TS structures were located using the default convergence criteria. However, some TS structures required stricter convergence criteria to obtain exactly one negative frequency. To verify the obtained structures are TS, visual inspection combined with measured Pd-C-Br bond lengths related to a TS structure under concerted mechanism and identification of exactly one negative frequency from the vibrational analysis are the requirements to confirm that the structure is indeed a TS structure. These frequencies are shown in Table A3 and Table A6 in Appendix A.

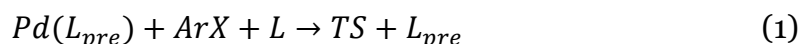
For Pd-complex containing axially chiral substrate and chiral ligand, namely substrate **9** and **10** and ligand **2**, **4** and **5**, there were 4 structures for each of the complexes to be investigated. For substrate **9** and **10**, there were two possible locations on the aryl halide for the OA reaction to occur, the two Br atoms, combining with the chiral ligand, yielded 2 transition states enantiomers from the OA reacting via re- or si-face and the other 2 with atropisomers from rotating naphthalene group. This totals to 2 pairs of enantiomers with each pair containing atropisomers. To evaluate which of the configurations are the minima structure, the energy calculation was performed for all the 2 pairs of enantiomers of the TS structures as shown in Table A5 in Appendix A, where the lowest energy configuration is used to calculate the lowest energy barrier. For the investigation of steric effects on reactivity, the structures with the lowest energy barrier with solvation effects accounted for are reported as shown in Table 1, with graphical diagram shown in Figure A1 in Appendix A.

**Table 1.** Relative energy barrier of TS structures for ligands **1-5** and substrate **6-10** in kcal/mol with PBE0-D3(BJ) level of theory, including solvents effects with THF. The  $\text{Substrate}_{\text{mean}}$  and  $\text{Ligand}_{\text{mean}}$  indicate the mean value of each row and column, for comparison purposes. The mean value of substrate **8** and ligand **5** excluded the outlier of substrate **8** with ligand **5** shown in parenthesis.

		$\Delta G^{\ddagger}_{\text{soln}}$ (kcal/mol)					
		Ligand					
		<b>1</b>	<b>2</b>	<b>3</b>	<b>4</b>	<b>5</b>	$\text{Substrate}_{\text{mean}}$
Substrate	<b>6</b>	23.8	27.6	28.9	25.9	28.9	27.0
	<b>7</b>	21.3	23.2	25.9	23.5	23.5	23.5
	<b>8</b>	14.8	16.8	19.7	21.4	(6.1)	18.2
	<b>9</b>	11.9	22.3	15.5	23.0	15.9	17.7
	<b>10</b>	16.8	16.3	18.8	19.2	18.3	17.9
Ligand <sub>mean</sub>		17.7	21.2	21.8	22.6	21.7	N/A

### 3.3 Free energy profile of the transition states

To evaluate the reactivity of a reaction, an energy diagram was constructed with a starting point and TS structure to give an overall view of the reaction. In this case, the structures for reactant and product were not available due to the varying geometry and unpredictable cis-trans rearrangement of the reactant of the product which required a further analysis, which was not possible due to time constraint. Therefore, the reactivity of the reaction can be measured by the relative energy barrier between the starting point, i.e. the preactivated palladium complex for all the TS structures to be compared with, and the TS. As the starting point, using a common reference point for the starting point results in the calculated energy barrier to be relative to that starting point. This gives the reaction scheme as shown in Equation 1 where TS is the TS structure of Pd-complex including aryl halide and the phosphine ligand from the calculation, and  $L_{pre}$  is the ligands p-benzoquinone and 1,5-cyclooctadiene, coordinating the preactivated Pd-complex [Pd( $\eta^2$ : $\eta^2$ -p-benzoquinone)( $\eta^2$ : $\eta^2$ -1,5-cyclooctadiene)] with the structure shown in Figure B1 in Appendix B. The total free energy values of each ligand, substrate and preactivated Pd-complex are shown in Table A1 in Appendix A and are used for calculation according to reaction scheme in Equation 1.



Relating the starting point to the transition state is done using Equation 2 where  $\Delta G_{solv}^\ddagger$  is the relative energy barrier with solvation effects partially accounted for;  $\Delta G_{solv}^{TS}$  and  $\Delta G_{solv}^{start}$  are the terms which describes the solvation free energy of the transition state structure and the starting geometry.

$$\Delta G_{solv}^\ddagger = \Delta G_{solv}^{TS} - \Delta G_{solv}^{start} \quad (2)$$

To obtain the  $\Delta G_{solv}^{TS}$  and  $\Delta G_{solv}^{start}$ , these can be calculated for each of the structures by using equation 3. In equation 3,  $\Delta G$  is the total Gibbs free energy where the translational, rotational and vibrational energy is accounted for, although these contributions are calculated with the structure in gas phase. Therefore, in this study, the contributions from these molecular motion in gas phase are assumed in this calculation to be the same as in solution phase. As for  $\Delta E_{solv}$ , the term describes the difference between gas phase energy and solution phase energy, which is the solvation energy deriving from the process of simulating solvation of the structure with, in this case, THF solvent. The value for  $\Delta E_{solv}$  is shown in Table A1 and A4 in Appendix A.

$$\Delta G_{solv} = \Delta G + \Delta E_{solv} \quad (3)$$

Computing each combination of substrate and ligand yields the relative energy barrier shown in Table 1. The energy barrier is shown to slightly decrease for substrate **6-7** and the drastically decrease for other substrates with the introduction of biaryl substrates. This indicates that the reactivity increases when the steric bulk of the substrate increases. Although the trend for the ligand is difficult to generalize. So, to

pinpoint the component which affects the reaction, the ligands and substrates are evaluated separately.

### 3.3.1 Ligand's steric effects

The ligand steric effects have been shown to be an important factor in reactivity of cross-coupling reactions [4][26] where bulkier ligand can increase the rate of the cross-coupling reactions. However, the steric effects of the ligand are shown to be contributing to cross-coupling reactions in its entirety of the catalytic cycle including transmetalation and reductive elimination step. Additionally, bulkier ligand can affect the resulting TS structures, where the size of ligand can determine the number of ligands that can bind to the Pd. Smaller ligand such as ligand **1** allows the coordination of two ligands onto the Pd atom, whereas larger ligand such as ligand **5** is sterically possible for the coordination of only one ligand onto the Pd atom. The steric effects contribution to OA can be shown in the results obtained in this study. Although, for the model system to be consistent, the TS structures in this study are structures where only one ligand is coordinated to the Pd atom.

Upon examining the results obtained, it is shown that across the energy barriers of ligands used in this study, there was a slight change in the barrier with the increasing size of the ligand. Also, there is a trend that can be seen where the energy barrier is generally the lowest for ligand **1** and tends to increase with the increasing size of the ligand. Ligand **3** and **4** energy barrier is generally higher than the rest of the ligands. Also, ligand **5** did not follow the expected trend being that the energy would increase, which was attributed to the outlier of substrate **8** ligand **5** and the overall decrease in energy barrier for substrate **9** and **10** for ligand **5**. The relative energy barrier of this structure is significantly lower than all the structures in the series, at 6.1 kcal/mol.

This could be due to the computational method where during the transition state search, the differing convergence conditions for DFT-calculation of electronic energy were required as some of the transition state structures were difficult to identify. This led to a finer calculation which overestimated the electronic energy of the structure. Furthermore, by inspecting the solvation energy for substrate **8** ligand **5** compared to other structures in Table A4 in Appendix A, one can see that the problem arises from the solvation energy calculation. This is a consequence of calculation not converging properly, resulting in abnormal calculated electronic energy of the structure. To further confirm this, Figure 3 shows the comparison between the structure of substrate **8** ligand **4** and substrate **8** ligand **5** which showed that the geometry did not differ significantly, yet the energy barrier differs by 15.3 kcal/mol. Which further indicates that the fault lies in the electronic energy calculation. For this reason, this outlier is excluded from the analysis in this study.

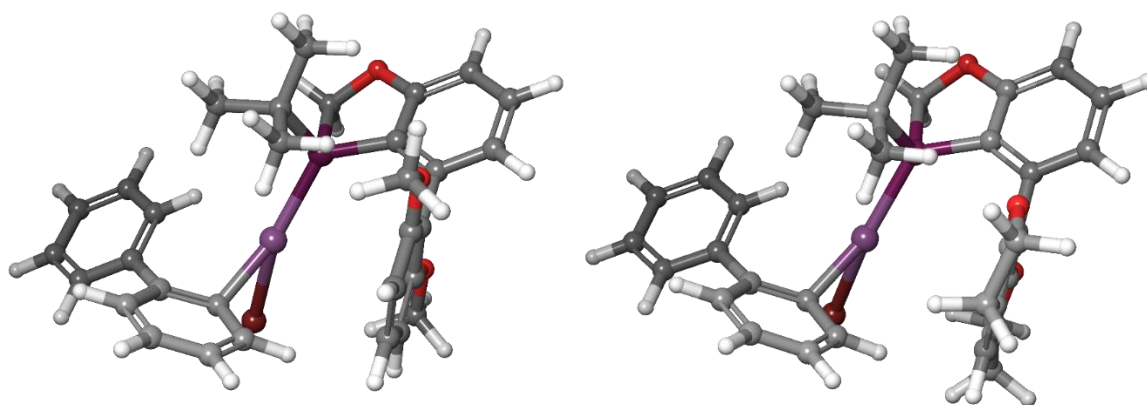


**Figure 3.** Geometrical comparison between the TS structure of substrate **8** ligand **4** (left) and substrate **8** ligand **5** (right).

Investigating the solvent contribution to the transition state structures, it was shown in Table A4 in Appendix A that the contribution from THF solvent increases from ligand **1** to **5**, where ligand **4** and **5** was shown to have a positive interaction with THF as a solvent as the solvation energy, as shown in Table A4, for the two ligands are comparatively lower than the first three ligands across all the substrates. This shows that the solvent stabilizes ligand **4** and **5** more effectively than ligand **1-3**. This could be due to the polarity of THF as it is a slightly polar solvent which combined with comparatively polar nature of ligand **4** and **5**, led to a decrease in the energy barrier. Although, to fully confirm this, different solvents with varying polarity are required to fully elucidate the extent of solvent effects.

Further inspection of the TS structures for ligand **2**, **4** and **5** shows a possible interaction between the ligand and the palladium atom. This is only seen in ligand **2**, **4** and **5** where the O atom of the biphenyl is in the proximity of Pd atom. This shows that there is a possibility where a ligand can hinder the Pd coordination site as shown in Figure 4.

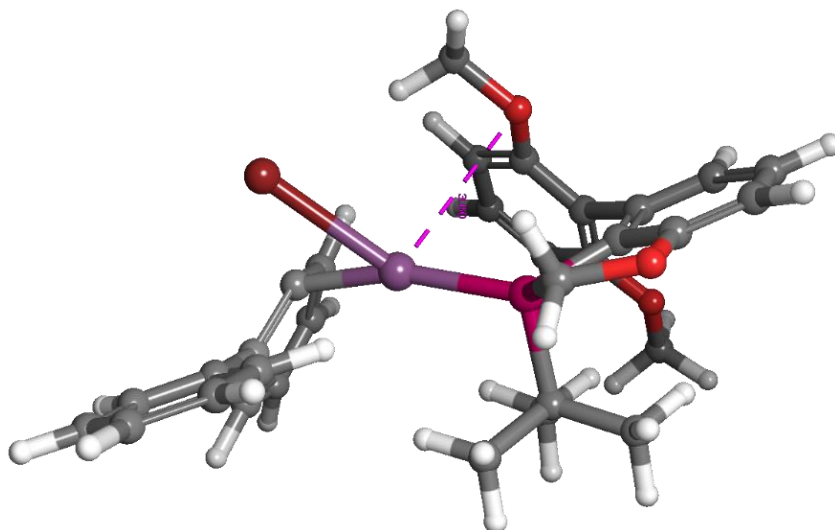


**Figure 4.** Modelling of Pd-complex of substrate **8** and ligand **4** with atomic distances between the interacting atoms, O atom and Pd atom, displayed.

Due to this reason, the ligands which can hinder a coordination site of Pd and the ligands that cannot, i.e. ligands **1** and **3** in this study, are not comparable due to the two diverging mechanisms of action. Where for ligands **1** and **3**, for the results to be comparable, the coordination site of Pd must be in proximity to another ligand. But as the structure of ligands **2**, **4** and **5** are not in proximity to the Pd atom, resulting in less hindered Pd center, the results will therefore be incomparable. This resulted in the low energy structures with ligand **2**, **4** and **5** where this could have been attributed to the more stable complex with open coordination site.

In this case, the reported energy barrier indicated that the steric effect of the ligand did not lead to a decrease in energy barrier and instead increases it. This could be due to the ligand steric effect as larger ligands can prevent additional ligand or solvent molecules to interact with the complex, therefore preventing the complex to adopt the stable geometry. However, this could not be confirmed as the two types of ligands were not comparable due to their difference in the ability to interfere with coordination of Pd center. But due to the time constraints, this option was not possible, as to obtain a full comprehensive comparative study, larger selections of ligands were required resulting in more calculations for all the TS complex structures.

Beside the coordination interfering effect of ligand, the electron donating capability of the ligand was shown by previous studies to be a contributing factor to facilitate OA reaction [14]. Relating the findings to the previous studies, as Landeros et al. [13] investigated ligand steric properties, the results for bromobenzene were that the steric bulk of the ligand did not affect the OA reaction considerably. The study varies the coordination number of the Pd complex, thus relating the coordination number to the steric properties to investigate the rate of the reaction. The reaction was nearly zeroth-order reaction for different coordination number of Pd complex with aryl bromide which means that the reaction depends on the substrate concentration and not the

coordination number of the Pd center, i.e. the steric properties of the ligand. They further highlighted that OA reaction depends largely on the identity of the halide, showing that the electronic effects could be the predominant factor in the reactivity of OA. Additionally, Jover et al. [14] did a computational study of phosphine ligand and its effects in SM cross-coupling reaction. It was stated that the OA step is dictated by primarily the ligand's electronic effects and minimally on ligand steric effects. The multilinear regression model deriving from HOMO energy and steric descriptors was constructed and shown that the HOMO energy describing the ligand's ability to donate electrons to Pd, in other words, the electronic effects, had much larger contribution than the steric descriptors on reactivity of OA.

To briefly investigate the electronic effects, the atomic charges, deriving from the electrostatic potential from DFT-calculation, of the important atoms participating in the reaction can be inspected. This is shown in Table A7 in Appendix A for each of the ligand/substrate combinations, highlighting the interacting atoms in the reaction. In the case of the ligand, the atomic charge of Pd atoms in the structures were shown to follow the same trend for ligand **1-5** as the reported energy barrier. Where the atomic charge of Pd atom increases, i.e. becomes more positively charged, due to the varying electronic structure of the ligands, relating the nucleophilicity of Pd atom to the reactivity of the OA reaction. Furthermore, looking at the phosphine ability to donate electrons to Pd by inspecting the atomic charge of P atoms, it is shown that the phosphine of ligand **2-5** retains some of its electrons rather than donating it all to Pd atom. This indicates that the ligands are strongly electron donating ligands as the some of the electron density is retained on the P atom while most of it is present on Pd atom as the atomic charge of Pd atoms in Table A7 indicated.

So, while the trend of ligand's steric effects indicates that the increase in steric bulk of ligand leads to a decrease in reactivity of OA reaction which could be due to the coordination site interference from the ligand, there were many signs which indicate that the steric bulk is not the sole contributor to reactivity of OA. Two of which are solvent effects and electronic effects. For solvent effects, the choice of solvent can change depending on the choice of ligand and substrates since the polarity of solvent can facilitate the stabilization of the complex. As for electronic effects, the ligand's electron donating ability is important for the reactivity as strongly electron donating ligand led to Pd atom becoming more nucleophilic, leading to an increase in reactivity. Although, a further analysis into the electronic effects is required as the model system of this study is focused on studying the steric effects and therefore could not elucidate the full extent of how electronic effects of the ligand can affect the reactivity of OA reaction.

### **3.3.2 Substrate's steric effects**

The substrates used in this study contain substituents with varying degrees of steric bulk in the ortho position to the reaction center and thus will be in the proximity to the Pd atom and possibly to the ligand during OA. Although, the substituent's steric bulk is not the metric used in this study to evaluate the substrate's steric effects.

Instead, to provide a description of what steric effects mean for Pd-complex, the steric effects which matter in this study are the steric effect which interacts with the rest of the complex in the transition state (TS), specifically those that collide with either the Pd center or the ligand.

As for the substrate steric effects, looking at the first substrate **6**, the energy barrier is shown to be higher than the bulkier substrates. Inspecting other substrates **7-10**, the energy barrier decreases with increasing steric bulk on the substituent, indicating that steric effect affects the reactivity of OA where increasing steric bulk will decrease the energy barrier. Therefore, to confirm the hypothesis, the results from this study can be tied to the results from other previous studies.

Recalling previous studies [15] where a reactivity model was constructed which is described by the linear regression coefficient of each descriptor, and it is shown that the model estimated the coefficient of the steric effect to be positive, indicating the increase in steric bulk of the substituent leads to an increase in energy barrier of the TS. The contribution of sterics descriptors to the energy barrier in the model was shown to be less than 10% as opposed to another descriptor such as electronics descriptor (>60%). This indicates that the trend in this study shown in Table 1 does not coincide with the trend in the study that Lu et al. showed, as the reported energy barrier of the study herein was shown to be decreasing with increasing steric bulk of the substituent.

The previous study by Lu et al. [15] however shows that the steric bulk of the substrate is not the main cause of affecting the reactivity of the OA reaction, as if it was the case, the energy barrier would be increasing with the increasing steric bulk as the steric descriptor coefficient indicated. Instead, the energy barrier decreases in the results shown in Table 1, suggesting that there are other factors which affect the OA reaction greater than steric effects. The consensus [15][16] of previous studies is that the substituent on the aryl halide substrate matters greatly when it is on the ortho position to the halide atom. This confirms the finding of previous studies that ortho-substituent does increase energy barrier of OA. As to why, the primary contributing factor for reactivity of OA is likely to be from electronic effects, not steric effects of the substrate. Ahlquist et al. [12] showed that having an electron withdrawing substituent at C<sub>para</sub> leads to a decrease in energy barrier since this enhances Pd ability to donate electron, therefore making the aryl halide substrate to be more electrophilic in nature. With the same rationale, having electron withdrawing substituent at C<sub>ortho</sub> will result in a decrease in energy barrier as the inductive effect of an electron withdrawing substituent promotes electrophilicity of the aryl halide, resulting in an increase in reactivity of OA reaction.

In this case, the trend in electronic effect of the substituents in the substrates used in this study can be estimated with the use of Hammett  $\sigma$  constant for para substituent and meta substituent [27] as shown in Table 2 to relate the finding of this study to the previous studies, where  $\sigma_{para}$  corresponds to the ortho substituents due to inductive effect. The negative value of Hammett  $\sigma$  constant indicates that the substituent is an

electron donating group to the aromatic ring while positive value indicates that the substituent is an electron withdrawing group. The results from this study do agree with the previous study as shown with all the substrates in the series. This showed that an electron withdrawing group at para/ortho position decreases the energy barrier as shown in substrate **7** to **8**. Although, an electron donating group with ortho-methyl as shown in substrate **6** to **7**, was expected to increase the energy barrier, instead the energy barrier decreases. This indicates that further study is required to investigate the full extent of the electronic effects and to explain the ortho-substituents inductive effects.

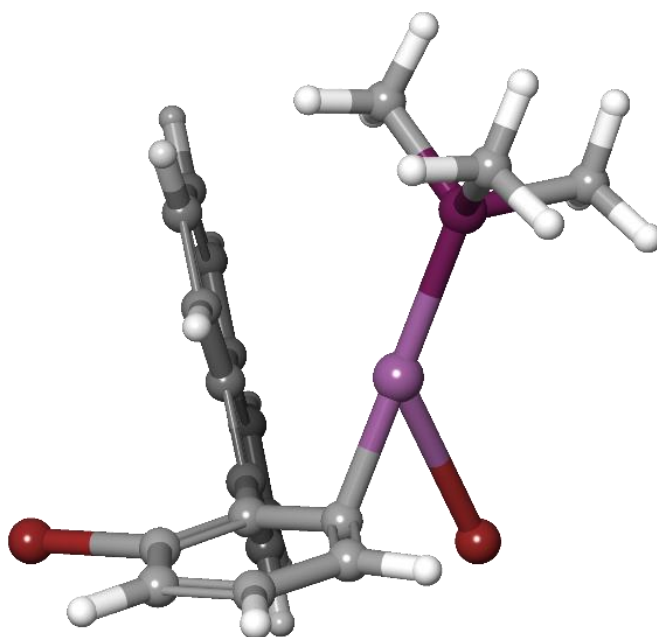


**Figure 5.** Modelling of Pd-complex of substrate **9** and ligand **1** showing the addition of Br at meta-position.

As for substrates **8** and **9/10**, the decrease in energy barrier differs considerably. In this case the bromide substituent must be considered for substrates **9** and **10** as shown for substrate **9** with ligand **1** in Figure 5. The  $\sigma$  constant for ortho substituent of substrates **9** and **10** showed that the ortho-naphthyl and ortho-2-methyl-naphthyl are comparable in their ability to withdraw electron which could not be the reason for the decrease in energy barrier for substrate **9** and **10** compared to the previous substrates in the series. Instead, the meta-bromide is thought to be responsible for the decrease in energy barrier as the  $\sigma$  constant showed that the meta-bromide is a stronger electron withdrawing group, correlating to the decrease in energy barrier.

**Table 2.** Estimated Hammett  $\sigma$  constant of the substituents in substrate **6-10**. Negative value indicates electron donating group and positive value indicates electron withdrawing group.

Substituent	Corresponding substrate	$\sigma_{\text{para}}$	$\sigma_{\text{meta}}$
<b>Ortho-H</b>	Substrate <b>6</b>	0	0
<b>Ortho-Methyl</b>	Substrate <b>7</b>	-0.148	-0.030
<b>Ortho-Phenyl</b>	Substrate <b>8</b>	0.012	0.055
<b>Ortho-Naphthyl</b>	Substrate <b>9</b>	0.015	0.078
<b>Ortho-2-Methyl-naphthyl</b>	Substrate <b>10</b>	-0.005	0.073
<b>Meta-Bromide</b>	Substrates <b>9</b> and <b>10</b>	0.282	0.392

While the Hammett  $\sigma$  constant is shown to be a good estimation, it is important to investigate electronic effects further to show if the addition of substituents resulted in the decrease in energy barrier due to steric effect or the electronic effects. This can be done by combining the estimated Hammett  $\sigma$  constant to compare with the atomic charges of interacting atoms in the reaction shown in Table A7 in Appendix A for the substrate and the participating atoms. This shows that for the substrates, the atomic charge of Pd atom increases with increasing steric bulk of the substrate, leading to Pd atom becoming less nucleophilic along the series of substrates. Similarly for the interacting carbon atom,  $C_{\text{ipso}}$ , the atomic charge decreases with increasing steric bulk of the substrate, leading to the  $C_{\text{ipso}}$  atom becoming less electrophilic along the series of substrates. Therefore, it is shown that increasing the steric bulk from substrate **6-10** should lead to an increase in energy barrier as the Pd atom and  $C_{\text{ipso}}$  become less nucleophilic and electrophilic respectively. However, this is not the case for the reported energy barrier, as the energy barrier was shown to decrease in this study. This could be due to the charge distribution which occurs during the TS, where the nucleophile donates electrons, resulting in the increased atomic charge of Pd atom and vice versa for electrophilic  $C_{\text{ipso}}$  atom. This shows that the degree of charge distribution during TS could be correlated with the energy barrier, where the larger substrates and its electron withdrawing substituents promote the electrons to be redistributed more effectively. This results in Pd atoms becoming more positively charged and  $C_{\text{ipso}}$  becoming more negatively charged and therefore decreasing the energy barrier as the steric bulk increases for substrate **6-10**. Although, to fully understand how the charge distribution in the structure during TS occurs, a deeper investigation and validation is required.

Besides the inductive effects, there is further evidence confirming that steric effects do affect reactivity shown in the TS structure substrate **9** and **10**, This is related to the coordination site interference which can be shown in Figure 6. As discussed in the previous section with ligand steric effects, the O atom in ligand **2**, **4** and **5** was shown to hinder the coordination site, resulting in decrease in energy barriers. For the case of substrate **9** and **10**, similar situation arises as the naphthalene substituent is bulky enough to be in the proximity of the Pd center as shown in Figure B17-B26 in Appendix B and therefore could be the reason the energy barrier decreases for these substrates.

This finding is not consistent with the previous study as Lu et al. [15] stated that the increase in steric bulk of the substituent leads to an increase in energy barrier of the TS structure.

However, the substrates used in the previous study contained substituents (R = -H, -methyl, -ethyl, -isopropyl, -tertbutyl), none of which, beside tertbutyl, is large enough to be in proximity to the coordination site of Pd due to its relatively smaller steric bulk near Pd center. The case can be made for tertbutyl substituent to have the ability to interfere with the coordination site as tertbutyl group is comparable in size to the substituents of substrates **8-10** in the current study. But, as the study by Lu et al. evaluated the substituents altogether to derive the coefficient of steric descriptor, the steric effects of tertbutyl was possibly overshadowed by the smaller substituents. Also, the substituents used in the model were either ortho- or para-substituents as opposed to strictly ortho-substituents used in this current study. This ultimately led to the model equation for steric descriptor in the study by Lu et al. being inconsistent and therefore incomparable to the finding in this study. However, substrate **9** and **10**, with the atropisomer formed, their TS structures were all shown to have naphthyl substituents oriented towards the ligand with P-configuration. This orientation results in substrate being in proximity to the coordination site of the Pd-complex and might contribute to the decrease in energy barrier due to steric effects. Although, as there were also indications that electronic effect could affect the reactivity, it is unclear whether the steric effect or the electronic effect is the dominating factor to affect reactivity.

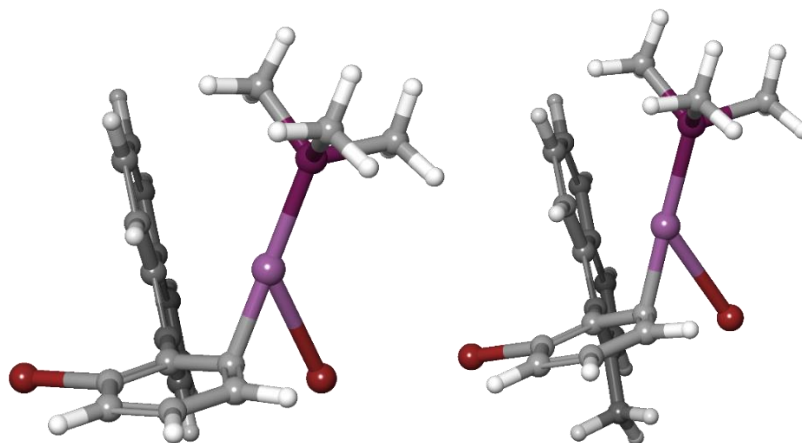


**Figure 6.** Modelling of Pd-complex of substrate **9** and **10** and ligand **1** showing interference of coordination site from the substrate's substituent.

As the steric effects were shown to affect the reactivity when the substrates are bulky enough to be in the proximity of the coordination site, further investigations regarding steric effects are needed until the electronic effect study on OA is confirmed to not be the main factor on the set of substrates and ligands used in this study. Hence, to elucidate whether the electronic effect was the factor which decreases the energy barrier or if it was the steric effect, a further assessment on the electronic effect and the coordination site interference is needed.

## 4 Conclusion

---

The steric features of both ligand and substrate were investigated, as for the ligands included and compared in this study, the steric bulk of the ligands were shown to have a small effect on the reactivity where increasing the ligand size resulted in an increase in the energy barrier. This was shown to be due to the ligand's structure as some larger ligand can interfere with the Pd center by being in proximity to it. Other possible factors were also considered, such as solvent and electronic effects. However, the model used in this study was not aimed at studying said effects and therefore, the conclusion that solvent and electronic effects do affect OA reactivity cannot be drawn.

As for the substrate, an opposite trend can be seen where an increase in substrate size results in a decrease in the energy barrier. It is shown that the ortho-substituent causes the energy barrier to decrease. This could also be due to the electronic effects of the substituent where electron withdrawing group can cause the aryl halide to be more reactive, similarly with inductive effects of the substituents depending on the position of the substituent to the aryl. Additionally, the substrate's steric effects are shown to affect the reactivity of OA where the substrates that can interfere with coordination of Pd were shown to increase the reactivity of the reaction.

A limitation of this study is the exclusion of Pd complexes with multiple coordinated ligands, which may be lower in energy than the starting structure or TS included. The findings are theoretical and may not fully reflect real conditions. The study focuses on steric effects without accounting for ligand coordination, which could influence reactivity. So, for future studies, electronic features of the ligand and substrate should be considered alongside steric features where the substrates and ligands with the ability to affect the coordination site, both during and before TS, can be compared. This calls for a larger, focused selection of substrates and ligands to avoid possible interference to occur.

## **Acknowledgements**

---

I would like to take the last moment to give my warmest appreciation to my supervisor Christian Sköld for giving me the opportunity to develop my interests in computational chemistry, for taking your time to supervise and the insights which I gain during this project which I find to be invaluable. I would also like to extend my gratitude to Henning Henschel for all the constructive advice which helped me shape my project immensely. Lastly, I would like to give a shout out to the master thesis students during the Fall semester 2024 for all the lovely lunch breaks we've had.

## References

1. Brown, D. G., & Boström, J. (2016). Analysis of Past and Present Synthetic Methodologies on Medicinal Chemistry: Where Have All the New Reactions Gone? *Journal of Medicinal Chemistry*, 59(10), 4443–4458. <https://doi.org/10.1021/acs.jmedchem.5b01409>
2. Buskes, M. J., & Blanco, M. J. (2020). Impact of cross-coupling reactions in drug discovery and development. *Molecules* 25(15). MDPI AG. <https://doi.org/10.3390/molecules25153493>
3. Jana, R., Pathak, T. P., & Sigman, M. S. (2011). Advances in transition metal (Pd,Ni,Fe)-catalyzed cross-coupling reactions using alkyl-organometallics as reaction partners. In *Chemical Reviews* (Vol. 111, Issue 3, pp. 1417–1492). <https://doi.org/10.1021/cr100327p>
4. Barder, T. E., Walker, S. D., Martinelli, J. R., & Buchwald, S. L. (2005). Catalysts for Suzuki-Miyaura coupling processes: Scope and studies of the effect of ligand structure. *Journal of the American Chemical Society*, 127(13), 4685–4696. <https://doi.org/10.1021/ja042491j>
5. Hedouin, G., Hazra, S., Gallou, F., & Handa, S. (2022). The Catalytic Formation of Atropisomers and Stereocenters via Asymmetric Suzuki-Miyaura Couplings. In *ACS Catalysis* (Vol. 12, Issue 9, pp. 4918–4937). American Chemical Society. <https://doi.org/10.1021/acscatal.2c00933>
6. Norman, J. P., Larson, N. G., & Neufeldt, S. R. (2022). Different Oxidative Addition Mechanisms for 12- and 14-Electron Palladium(0) Explain Ligand-Controlled Divergent Site Selectivity. *ACS Catalysis*, 12(15), 8822–8828. <https://doi.org/10.1021/acscatal.2c01698>
7. Joshi, C., Macharia, J. M., Izzo, J. A., Wambua, V., Kim, S., Hirschi, J. S., & Vetticatt, M. J. (2022). Isotope Effects Reveal the Catalytic Mechanism of the Archetypical Suzuki-Miyaura Reaction. *ACS Catalysis*, 12(5), 2959–2966. <https://doi.org/10.1021/acscatal.1c05802>
8. Rio, J., Liang, H., Perrin, M. E. L., Perego, L. A., Grimaud, L., & Payard, P. A. (2023). We Already Know Everything about Oxidative Addition to Pd(0): Do We? In *ACS Catalysis* (Vol. 13, Issue 17, pp. 11399–11421). American Chemical Society. <https://doi.org/10.1021/acscatal.3c01943>
9. Kania, M. J., Reyes, A., & Neufeldt, S. R. (2024). Oxidative Addition of (Hetero)aryl (Pseudo)halides at Palladium(0): Origin and Significance of Divergent Mechanisms. *Journal of the American Chemical Society*, 146(28), 19249–19260. <https://doi.org/10.1021/jacs.4c04496>
10. Crabtree, R. H. (2005). *The Organometallic Chemistry of the Transition Metals*, 4th ed., pp. 166–169. John Wiley & Sons, Inc. Print ISBN:9780471662563 Online ISBN:9780471718765 <https://doi.org/10.1002/0471718769.fmatter>
11. Ahlquist, M., Fristrup, P., Tanner, D., & Norrby, P. O. (2006). Theoretical evidence for low-ligated palladium(0): [Pd-L] as the active species in oxidative addition reactions. *Organometallics*, 25(8), 2066–2073. <https://doi.org/10.1021/om060126q>
12. Ahlquist, M., & Norrby, P. O. (2007). Oxidative addition of aryl chlorides to monoligated palladium(0): A DFT-SCRF study. *Organometallics*, 26(3), 550–553. <https://doi.org/10.1021/om0604932>
13. Barrios-Landeros, F., Carrow, B. P., & Hartwig, J. F. (2009). Effect of ligand steric properties and halide identity on the mechanism for oxidative addition of haloarenes to trialkylphosphine Pd(0) complexes. *Journal of the American Chemical Society*, 131(23), 8141–8154. <https://doi.org/10.1021/ja900798s>

14. Jover, J., Fey, N., Purdie, M., Lloyd-Jones, G. C., & Harvey, J. N. (2010). A computational study of phosphine ligand effects in Suzuki-Miyaura coupling. *Journal of Molecular Catalysis A: Chemical*, 324(1–2), 39–47. <https://doi.org/10.1016/j.molcata.2010.02.021>
15. Lu, J., Donneck, S., Paci, I., & Leitch, D. C. (2022). A reactivity model for oxidative addition to palladium enables quantitative predictions for catalytic cross-coupling reactions. *Chemical Science*, 13(12), 3477–3488. <https://doi.org/10.1039/d2sc00174h>
16. Raders, S. M., Moore, J. N., Parks, J. K., Miller, A. D., Leibing, T. M., Kelley, S. P., Rogers, R. D., & Shaughnessy, K. H. (2013). Trineopentylphosphine: A conformationally flexible ligand for the coupling of sterically demanding substrates in the Buchwald-Hartwig amination and Suzuki-Miyaura reaction. *Journal of Organic Chemistry*, 78(10), 4649–4664. <https://doi.org/10.1021/jo400435z>
17. Alami, M., Amatore, C., Bensalem, S., Choukchou-Brahim, A., & Jutand, A. (2001). Kinetics of the oxidative addition of ortho-substituted aryl halides to palladium(0) complexes. *European Journal of Inorganic Chemistry*, 10, 2675–2681. [https://doi.org/10.1002/1099-0682\(200109\)2001:10<2675::aid-ejic2675>3.0.co;2-j](https://doi.org/10.1002/1099-0682(200109)2001:10<2675::aid-ejic2675>3.0.co;2-j)
18. Cao, Y.; Balduf, T.; Beachy, M. D.; Bennett, M. C.; Bochevarov, A. D.; Chien, A.; Dub, P. A.; Dyall, K. G.; Furness, J. W.; Halls, M. D.; Hughes, T. F.; Jacobson, L. D.; Kwak, H. S.; Levine, D. S.; Mainz, D. T.; Moore, K. B.; Svensson, M.; Videla, P. E.; Watson, M. A.; Friesner R. A., “Quantum chemical package Jaguar: A survey of recent developments and unique features”, *J. Chem. Phys.* 2024, 161(5), 052502
19. Bochevarov, A. D.; Harder, E.; Hughes, T. F.; Greenwood, J. R.; Braden, D. A.; Philipp, D. M.; Rinaldo, D.; Halls, M. D.; Zhang, J.; Friesner, R. A., “Jaguar: A high-performance quantum chemistry software program with strengths in life and materials sciences”, *Int. J. Quantum Chem.*, 2013, 113(18), 2110–2142
20. Gahlawat, S., Artelsmair, M., Castro, A. C., Norrby, P. O., & Hopmann, K. H. (2024). Computational Study of the Ir-Catalyzed Formation of Allyl Carbamates from CO<sub>2</sub>. *Organometallics*, 43(17), 1818–1826. <https://doi.org/10.1021/acs.organomet.4c00177>
21. David Rinaldo, Li Tian, Jeremy N. Harvey, Richard A. Friesner; Density functional localized orbital corrections for transition metals. *J. Chem. Phys.* 28 October 2008; 129 (16): 164108. <https://doi.org/10.1063/1.2974101>
22. Takahashi Y, Yamamoto Y, Katagiri K, Danjo H, Yamaguchi K, Imamoto T. P-chiral o-phosphinophenol as a P/O hybrid ligand: preparation and use in Cu-catalyzed asymmetric conjugate addition of diethylzinc to acyclic enones. *J Org Chem.* 2005 Oct 28;70(22):9009-12. doi: 10.1021/jo051034y. PMID: 16238340. A General and Special Catalyst for Suzuki–Miyaura Coupling Processes
23. Patel, N. D., Sieber, J. D., Teyrulnikov, S., Simmons, B. J., Rivalti, D., Duvvuri, K., Zhang, Y., Gao, D. A., Fandrick, K. R., Haddad, N., Lao, K. S., Mangunuru, H. P. R., Biswas, S., Qu, B., Grinberg, N., Pennino, S., Lee, H., Song, J. J., Gupton, B. F., ... Senanayake, C. H. (2018). Computationally Assisted Mechanistic Investigation and Development of Pd-Catalyzed Asymmetric Suzuki-Miyaura and Negishi Cross-Coupling Reactions for Tetra- ortho-Substituted Biaryl Synthesis. *ACS Catalysis*, 8(11), 10190–10209. <https://doi.org/10.1021/acscatal.8b02509>
24. Tang W., et al. (2010). A General and Special Catalyst for Suzuki–Miyaura Coupling Processes. . *Angewandte Chemie - International Edition*, 49(34), 5879–5883. <https://doi.org/10.1002/anie.201002404>

25. Kawamorita, S., Ohmiya, H., Iwai, T., & Sawamura, M. (2011). Palladium-catalyzed borylation of sterically demanding aryl halides with a silica-supported compact phosphane ligand. *Angewandte Chemie - International Edition*, 50(36), 8363–8366. <https://doi.org/10.1002/anie.201103224>
26. Walker, S. D., Barder, T. E., Martinelli, J. R., & Buchwald, S. L. (2004). A rationally designed universal catalyst for Suzuki-Miyaura coupling processes. *Angewandte Chemie - International Edition*, 43(14), 1871–1876. <https://doi.org/10.1002/anie.200353615>
27. Ertl, Peter. (2022). A Web Tool for Calculating Substituent Descriptors Compatible with Hammett Sigma Constants. *Chemistry–Methods*. 2(12), 2628–9725. <https://doi.org/10.1002/cmtd.202200041>

## Appendices

### APPENDIX A: Calculated energy of all substrates and ligands

**Table A1.** Calculated total free energy and solvation energy of isolated starting structures in the study in Hartree with PBE0-D3(BJ) level of theory, including solvents effects with THF.

Entry	Total free energy (Hartree)	Solvation energy (Hartree)
<b>Pd(L<sub>pre</sub>)</b>	-819.439745	-0.01624101902
<b>L<sub>pre</sub></b>	-692.642325	-0.01779779037
<b>Ligand 1</b>	- 460.768549	-0.00616502303
<b>Ligand 2</b>	- 884.421581	-0.01660173635
<b>Ligand 3</b>	- 1035.294113	-0.02039759131
<b>Ligand 4</b>	- 1303.56942	-0.02517726169
<b>Ligand 5</b>	- 1379.722651	-0.02647461708
<b>Substrate 6</b>	- 244.526916	-0.01509701917
<b>Substrate 7</b>	- 283.781064	-0.00766376288
<b>Substrate 8</b>	- 475.290534	-0.01137734158
<b>Substrate 9</b>	- 641.326771	-0.01744645597
<b>Substrate 10</b>	- 680.573653	-0.01797503382

Table A1 showed the calculated energy  $\Delta G$  and solvation energy  $\Delta E_{\text{solv}}$  through geometry optimization with vibration frequency analysis at  $T = 298.15$  K and  $P = 1$  atm. Note that Pd(L<sub>pre</sub>) is the preactivated Pd-complex [Pd( $\eta^2$ : $\eta^2$ -p-benzoquinone)( $\eta^2$ : $\eta^2$ -1,5-cyclooctadiene)] with the ligands L<sub>pre</sub> p-benzoquinone and 1,5-cyclooctadiene as shown in Figure B1 in Appendix B.

**Table A2.** Calculated total free energy of all compounds with its TS structures used in the reactivity study in Hartree with PBE0-D3(BJ) level of theory.

		Total free energy (Hartree)				
		Ligand				
		1	2	3	4	5
Substrate	6	-832.057765	- 1255.714543	- 1406.583405	- 1674.863703	- 1751.016458
	7	- 871.310911	- 1294.967635	- 1445.836709	- 1714.117295	- 1790.271872
	8	- 1062.823942	- 1486.481262	- 1637.349585	- 1905.630097	- 1981.783039
	9	- 1228.861955	- 1652.520487	- 1803.393421	- 2071.667499	- 2147.816687
	10	- 1268.116814	- 1691.778326	- 1842.648745	- 2110.921062	- 2187.076907

**Table A3.** Calculated lowest vibrational frequency and the intensity of all compounds with its TS structures used in the reactivity study in Hartree with PBE0-D3(BJ) level of theory, including solvents effects with THF.

Entry	Lowest vibrational frequency (cm <sup>-1</sup> )	Intensity (km/mol)
Lig 1 Sub 6	-108.8	137.9
Lig 1 Sub 7	-102.4	121.9
Lig 1 Sub 8	-124.0	165.5
Lig 1 Sub 9	-128.3	167.7
Lig 1 Sub 10	-128.3	165.9
Lig 2 Sub 6	-112.0	136.0
Lig 2 Sub 7	-101.3	112.5
Lig 2 Sub 8	-122.4	164.5
Lig 2 Sub 9	-128.9	165.1
Lig 2 Sub 10	-122.9	158.4
Lig 3 Sub 6	-103.8	124.5
Lig 3 Sub 7	-88.2	86.3
Lig 3 Sub 8	-108.5	131.6
Lig 3 Sub 9	-120.3	144.8
Lig 3 Sub 10	-117.9	135.9
Lig 4 Sub 6	-92.4	94.1
Lig 4 Sub 7	-68.2	71.3
Lig 4 Sub 8	-97.2	107.4
Lig 4 Sub 9	-91.0	90.0
Lig 4 Sub 10	-98.6	90.2
Lig 5 Sub 6	-89.4	84.2
Lig 5 Sub 7	-68.3	62.4
Lig 5 Sub 8	-79.2	85.3
Lig 5 Sub 9	-96.0	96.7
Lig 5 Sub 10	-80.9	73.1

**Table A4.** Calculated solvation energy of all compounds with its TS structures used in the reactivity study in Hartree with PBE0-D3(BJ) level of theory, including solvents effects with THF.

		Solvation energy (Hartree)				
		Ligand				
		1	2	3	4	5
Substrate	6	-0.01693340528	-0.01748290165	-0.02287523680	-0.02747036344	-0.02445421153
	7	-0.01449453249	-0.01816179446	-0.02108084133	-0.02450767254	-0.02441880548
	8	-0.02488751386	-0.02799341445	-0.03131430775	-0.02822208812	-0.05419996966
	9	-0.03390783588	-0.02227525567	-0.03652156424	-0.03046867830	-0.04712279369
	10	-0.01865695164	-0.02139609483	-0.02325439244	-0.03049539091	-0.03057518819

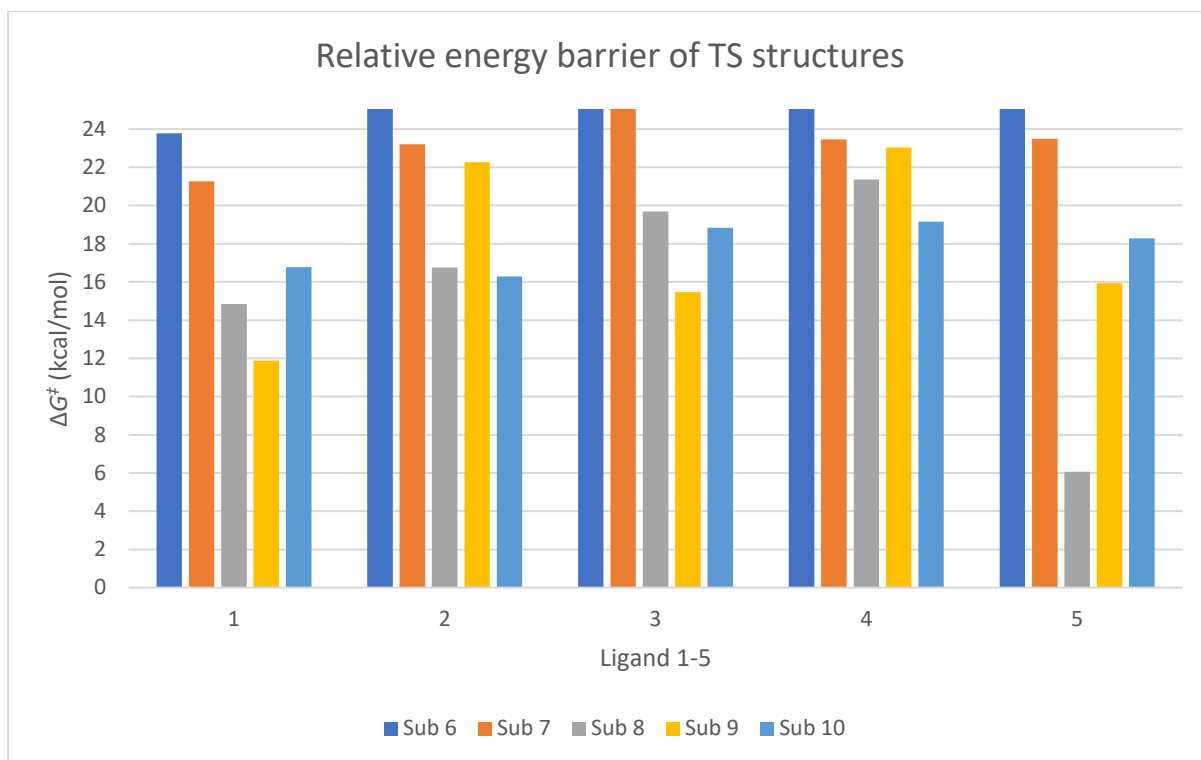


**Figure A1.** Diagram showing the relative energy barrier of TS structures used in reactivity in kcal/mol with PBEo-D3(BJ) level of theory, including solvents effects with THF.

**Table A5.** Calculated total free energy and solvation energy of all compounds used in evaluation of axially chiral structure in Hartree with PBE0-D3(BJ) level of theory, including solvents effects with THF. Note the configuration specified in the entry column, where the configuration of the ligand is denoted with R/S nomenclature and the configuration of the atropisomer is denoted with P/M nomenclature. The decimals are included as the difference in energy is not noticeable with one decimal.

<b>Entry</b>	<b>Total free energy (Hartree)</b>	<b>Solvation energy (Hartree)</b>
<b>Lig 2 Sub 9 (S,P)</b>	-1652.516452	-0.01447564899
<b>Lig 2 Sub 9 (S,M)</b>	-1652.520487	-0.02227525567
<b>Lig 2 Sub 9 (R,P)</b>	-1652.519222	-0.02336486503
<b>Lig 2 Sub 9 (R,M)</b>	-1652.517074	-0.02555380925
<b>Lig 4 Sub 9 (S,P)</b>	-2071.665002	-0.02994187488
<b>Lig 4 Sub 9 (S,M)</b>	-2071.666179	-0.03149180175
<b>Lig 4 Sub 9 (R,P)</b>	-2071.667499	-0.03046867830
<b>Lig 4 Sub 9 (R,M)</b>	-2071.665231	-0.03128162016
<b>Lig 5 Sub 9 (S,P)</b>	-2147.816687	-0.04712279369
<b>Lig 5 Sub 9 (S,M)</b>	-2147.819941	-0.03162954673
<b>Lig 5 Sub 9 (R,P)</b>	-2147.823708	-0.03265627529
<b>Lig 5 Sub 9 (R,M)</b>	-2147.817552	-0.03110299405
<b>Lig 2 Sub 10 (S,P)</b>	-1691.778326	-0.02139609483
<b>Lig 2 Sub 10 (S,M)</b>	-1691.773268	-0.02321692468
<b>Lig 2 Sub 10 (R,P)</b>	-1691.773517	-0.02329243154
<b>Lig 2 Sub 10 (R,M)</b>	-1691.770181	-0.02493176513
<b>Lig 4 Sub 10 (S,P)</b>	-2110.920911	-0.02968555627
<b>Lig 4 Sub 10 (S,M)</b>	-2110.918215	-0.03036595195
<b>Lig 4 Sub 10 (R,P)</b>	-2110.921062	-0.03049539091
<b>Lig 4 Sub 10 (R,M)</b>	-2110.92019	-0.02950423602
<b>Lig 5 Sub 10 (S,P)</b>	-2187.074886	-0.03030714906
<b>Lig 5 Sub 10 (S,M)</b>	-2187.071645	-0.03104108198
<b>Lig 5 Sub 10 (R,P)</b>	-2187.076907	-0.03057518819
<b>Lig 5 Sub 10 (R,M)</b>	-2187.074287	-0.02993255519

**Table A6.** Calculated lowest vibrational frequency and the intensity of all compounds with its TS structures used in evaluation of axially chiral structure in Hartree with PBE0-D3(BJ) level of theory, including solvents effects with THF. Note the configuration specified in the entry column, where the configuration of the ligand is denoted with R/S nomenclature and the configuration of the atropisomer is denoted with P/M nomenclature.

<b>Entry</b>	<b>Lowest vibrational frequency (cm<sup>-1</sup>)</b>	<b>Intensity (k/mol)</b>
<b>Lig 2 Sub 9 (S,P)</b>	-78.0	74.7
<b>Lig 2 Sub 9 (S,M)</b>	-68.2	71.3
<b>Lig 2 Sub 9 (R,P)</b>	-46.8	31.8
<b>Lig 2 Sub 9 (R,M)</b>	-72.8	76.9
<b>Lig 4 Sub 9 (S,P)</b>	-110.36	115.5
<b>Lig 4 Sub 9 (S,M)</b>	-113.6	123.4
<b>Lig 4 Sub 9 (R,P)</b>	-91.0	90.0
<b>Lig 4 Sub 9 (R,M)</b>	-91.9	100.3
<b>Lig 5 Sub 9 (S,P)</b>	-110.7	93.2
<b>Lig 5 Sub 9 (S,M)</b>	-105.7	109.9
<b>Lig 5 Sub 9 (R,P)</b>	-98.6	90.2
<b>Lig 5 Sub 9 (R,M)</b>	-103.7	100.6
<b>Lig 2 Sub 10 (S,P)</b>	-68.3	62.4
<b>Lig 2 Sub 10 (S,M)</b>	-79.5	80.0
<b>Lig 2 Sub 10 (R,P)</b>	-51.2	35.9
<b>Lig 2 Sub 10 (R,M)</b>	-83.6	80.8
<b>Lig 4 Sub 10 (S,P)</b>	-95.0	104.1
<b>Lig 4 Sub 10 (S,M)</b>	-112.4	114.2
<b>Lig 4 Sub 10 (R,P)</b>	-96.0	96.7
<b>Lig 4 Sub 10 (R,M)</b>	-94.4	96.8
<b>Lig 5 Sub 10 (S,P)</b>	-100.8	106.1
<b>Lig 5 Sub 10 (S,M)</b>	-106.4	109.6
<b>Lig 5 Sub 10 (R,P)</b>	-80.9	73.1
<b>Lig 5 Sub 10 (R,M)</b>	-90.6	96.2

**Table A7.** Atomic charges from electrostatic potential of the interacting atoms in concerted mechanism on the transition state structures of all compounds. Calculations were performed with PBE0-D3(BJ) level of theory.

Entry	Atomic charge			
	Pd	Br	P	Cipso
Lig 1 Sub 6	0.05772	-0.30393	0.26626	0.31740
Lig 2 Sub 6	0.27804	-0.28421	-0.34527	0.09073
Lig 3 Sub 6	0.29187	-0.30078	-0.53394	0.27496
Lig 4 Sub 6	0.37249	-0.29545	-0.65356	-0.23930
Lig 5 Sub 6	0.40632	-0.27151	-0.42359	-0.07420
Lig 1 Sub 7	0.06462	-0.28438	0.26259	0.15502
Lig 2 Sub 7	0.30276	-0.26247	-0.29571	-0.02103
Lig 3 Sub 7	0.36352	-0.29609	-0.77140	0.16229
Lig 4 Sub 7	0.36275	-0.29110	-0.64231	-0.08088
Lig 5 Sub 7	0.35174	-0.29038	-0.53979	-0.02465
Lig 1 Sub 8	0.05038	-0.30942	0.34522	0.31035
Lig 2 Sub 8	0.26251	-0.26579	-0.12727	-0.10381
Lig 3 Sub 8	0.31197	-0.29944	-0.52817	0.25050
Lig 4 Sub 8	0.35470	-0.29852	-0.49161	-0.03436
Lig 5 Sub 8	0.36522	-0.29464	-0.38672	-0.05382
Lig 1 Sub 9	0.13414	-0.22864	0.29441	-0.14375
Lig 2 Sub 9	0.35726	-0.20426	-0.28058	-0.63954
Lig 3 Sub 9	0.38809	-0.24602	-0.67713	-0.15141
Lig 4 Sub 9	0.49079	-0.25970	-0.75692	-0.43171
Lig 5 Sub 9	0.48728	-0.26618	-0.50271	-0.64288
Lig 1 Sub 10	0.15422	-0.25569	0.23847	-0.07911
Lig 2 Sub 10	0.36971	-0.21961	-0.31732	-0.53177
Lig 3 Sub 10	0.34526	-0.20065	-0.65634	-0.24230
Lig 4 Sub 10	0.52305	-0.24209	-0.77363	-0.78923
Lig 5 Sub 10	0.50954	-0.22044	-0.59100	-0.74234

## APPENDIX B: Modeling of all substrates, ligands and preactivation Pd-complex

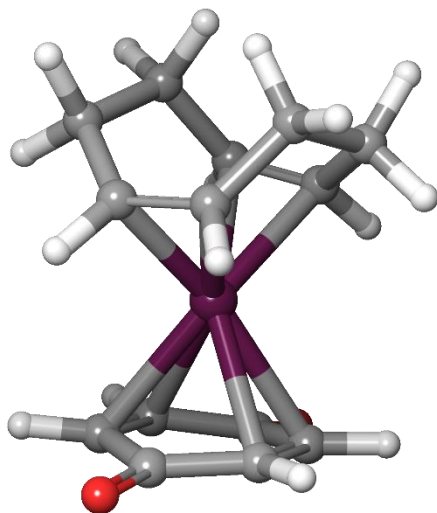


**Figure B1.** Modelling of preactivation Pd-complex containing 2 ligands with the identifier EJAJII in CCDC database.

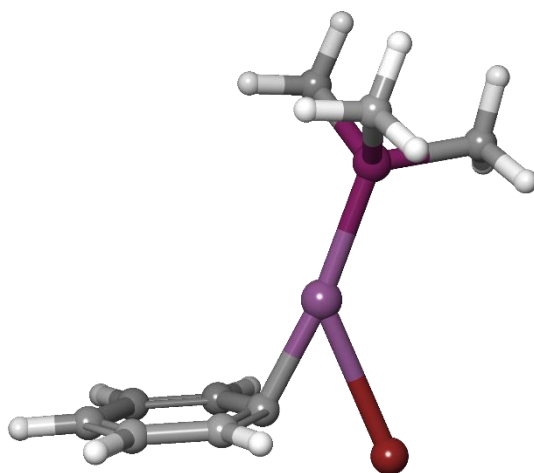


**Figure B2.** Modelling of Pd-complex of substrate **6** and ligand **1**.

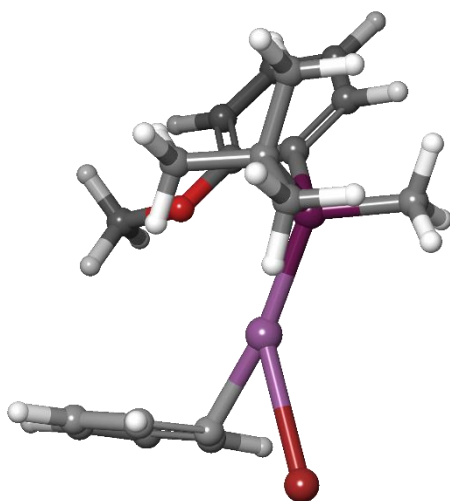


**Figure B3.** Modelling of Pd-complex of substrate **6** and ligand **2**.

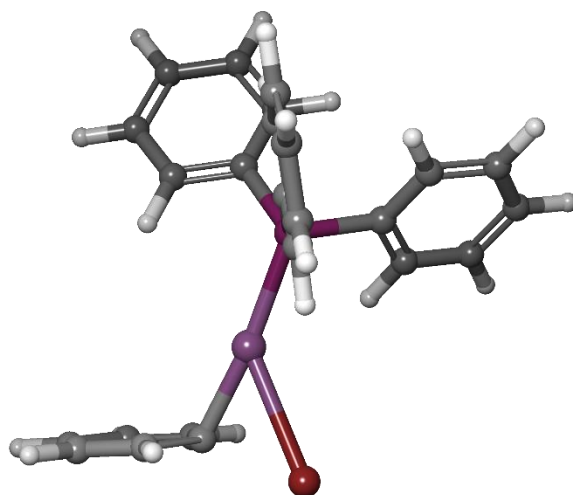


**Figure B4.** Modelling of Pd-complex of substrate **6** and ligand **3**.

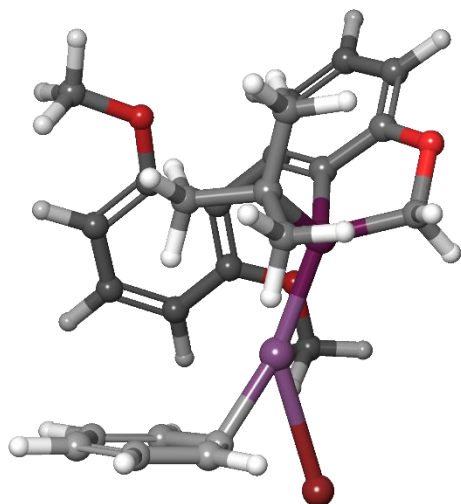


**Figure B5.** Modelling of Pd-complex of substrate **6** and ligand **4**.

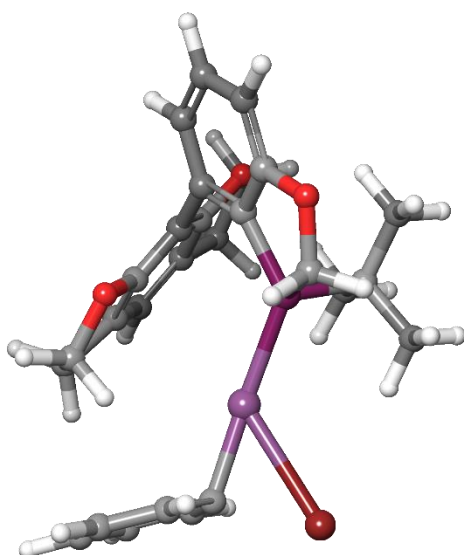


**Figure B6.** Modelling of Pd-complex of substrate **6** and ligand **5**.

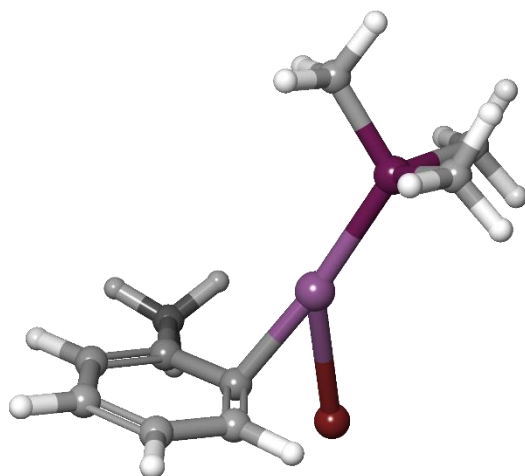


**Figure B7.** Modelling of Pd-complex of substrate **7** and ligand **1**.

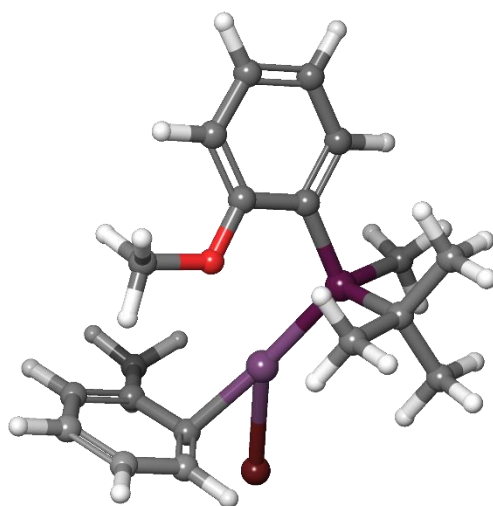


**Figure B8.** Modelling of Pd-complex of substrate **7** and ligand **2**.

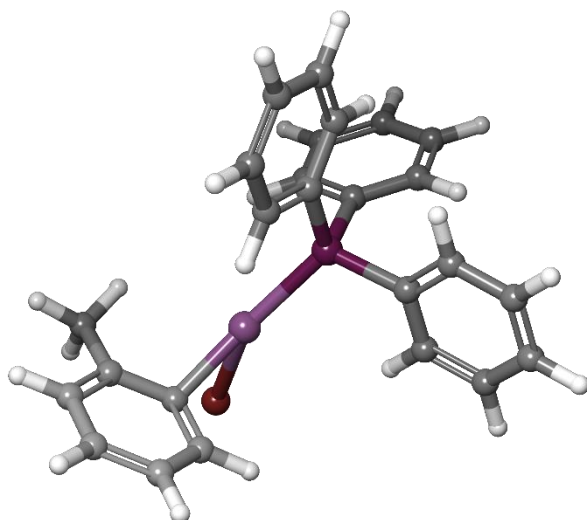


**Figure B9.** Modelling of Pd-complex of substrate **7** and ligand **3**.

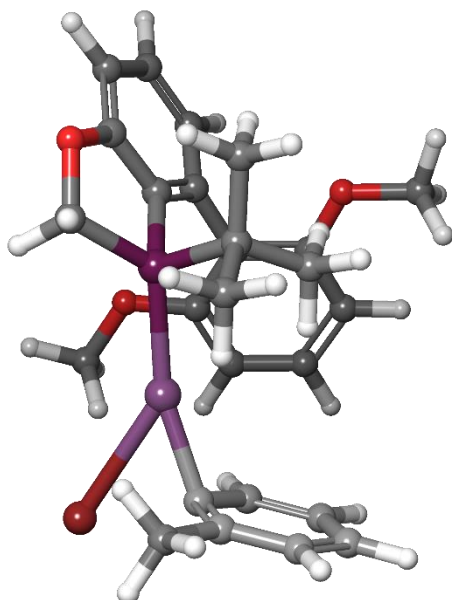


**Figure B10.** Modelling of Pd-complex of substrate **7** and ligand **4**.

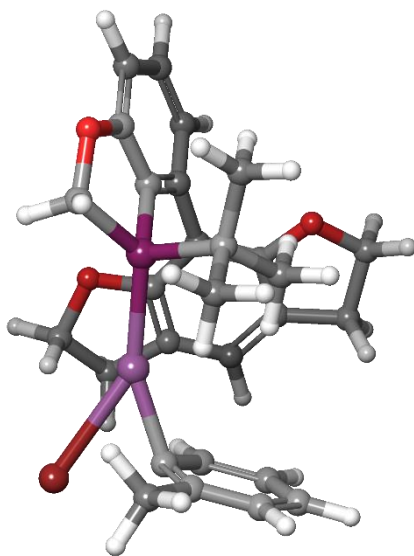


**Figure B11.** Modelling of Pd-complex of substrate **7** and ligand **5**.

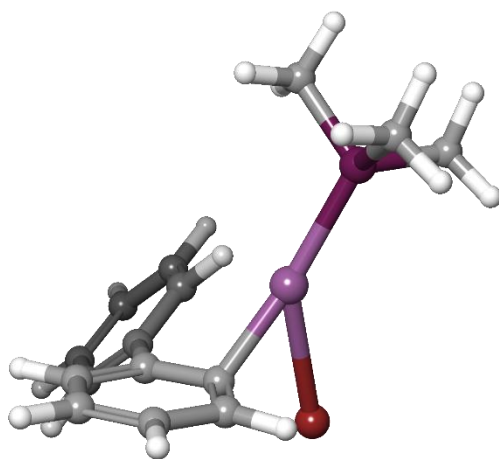


**Figure B12.** Modelling of Pd-complex of substrate **8** and ligand **1**.

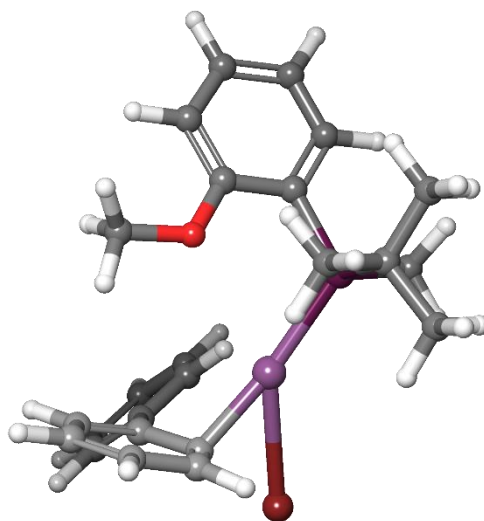


**Figure B13.** Modelling of Pd-complex of substrate **8** and ligand **2**.

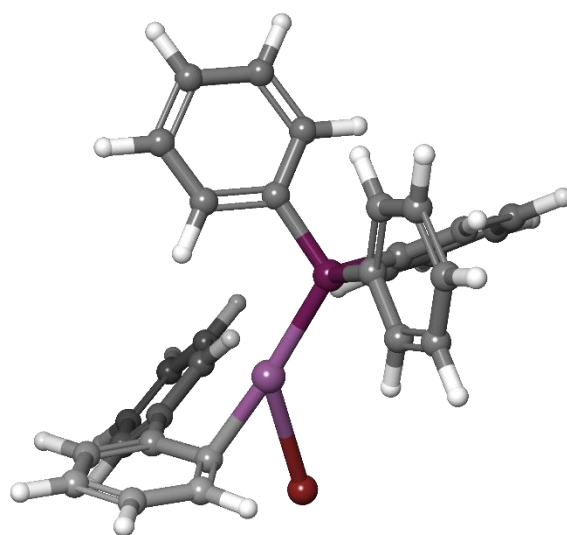


**Figure B14.** Modelling of Pd-complex of substrate **8** and ligand **3**.

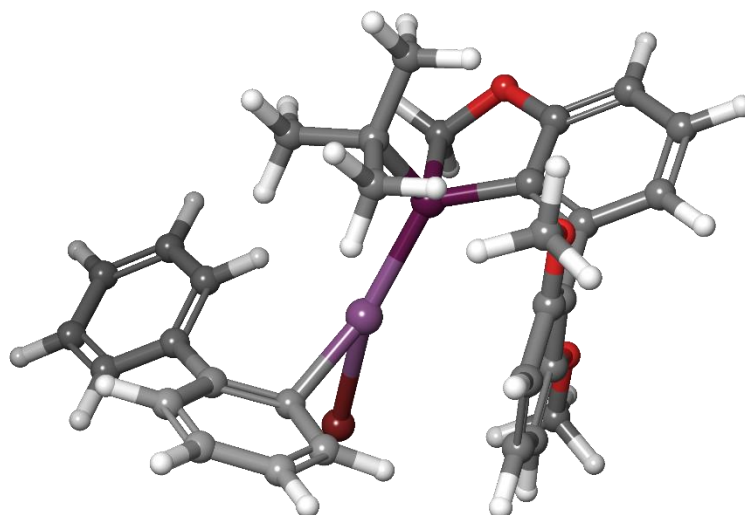


**Figure B15.** Modelling of Pd-complex of substrate **8** and ligand **4**.

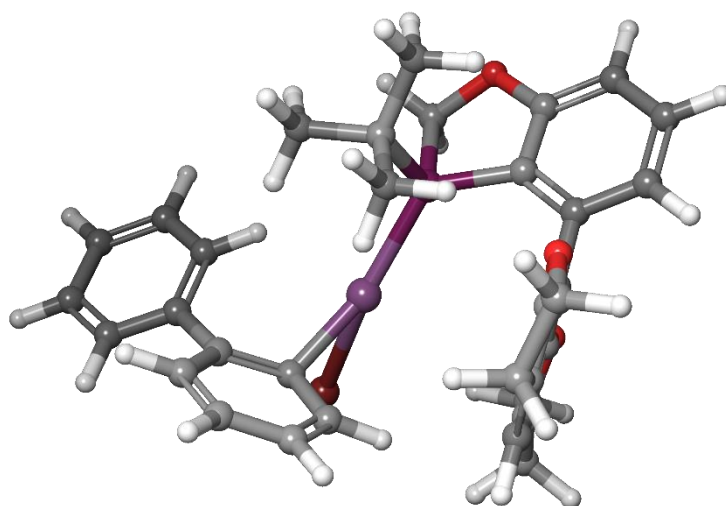


**Figure B16.** Modelling of Pd-complex of substrate **8** and ligand **5**.

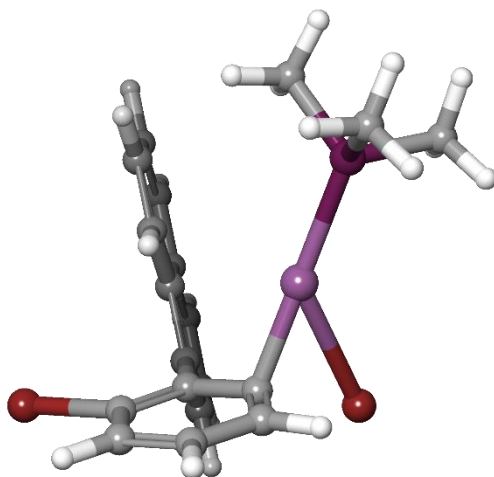


**Figure B17.** Modelling of Pd-complex of substrate **9** and ligand **1**.

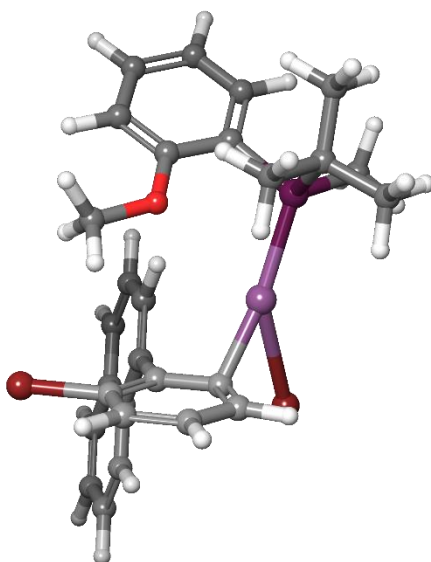


**Figure B18.** Modelling of Pd-complex of substrate **9** and ligand **2** with configuration (S,M).

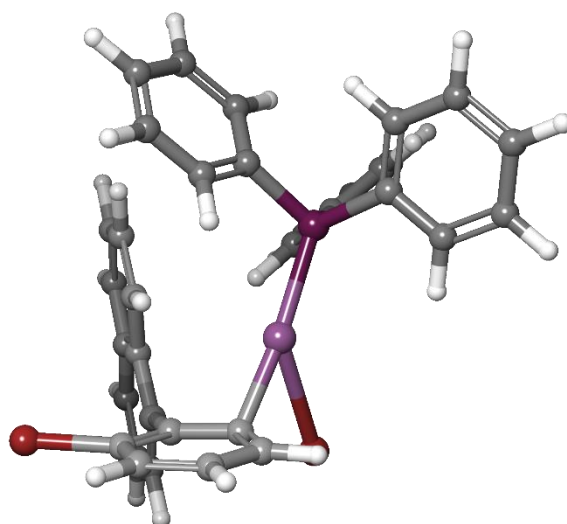


**Figure B19.** Modelling of Pd-complex of substrate **9** and ligand **3**.

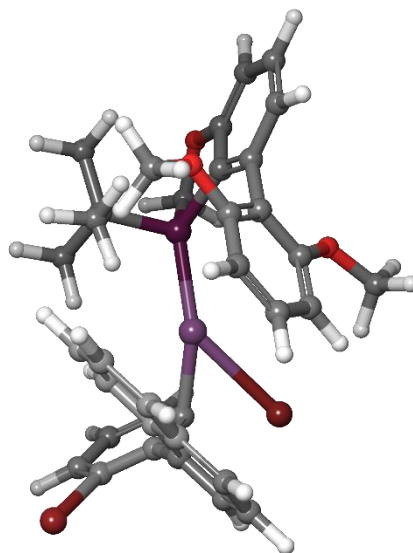


**Figure B20.** Modelling of Pd-complex of substrate **9** and ligand **4** with configuration (R,P).

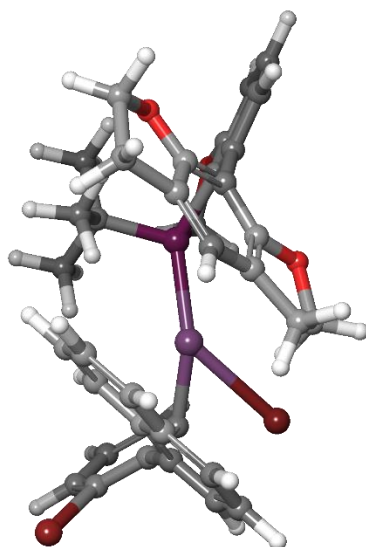


**Figure B21.** Modelling of Pd-complex of substrate **9** and ligand **5** with configuration (R,P).

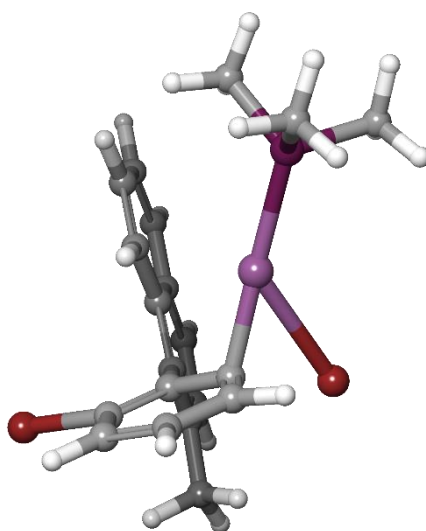


**Figure B22.** Modelling of Pd-complex of substrate **10** and ligand **1**.

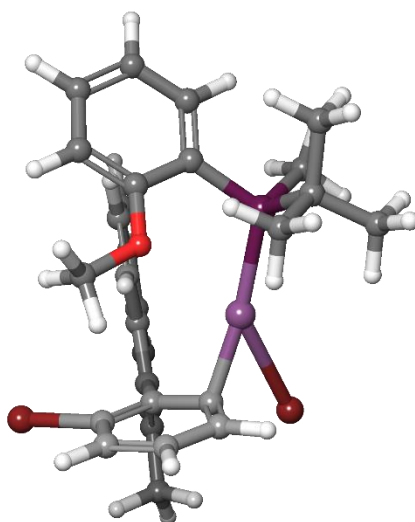


**Figure B23.** Modelling of Pd-complex of substrate **10** and ligand **2** with configuration (S,P).

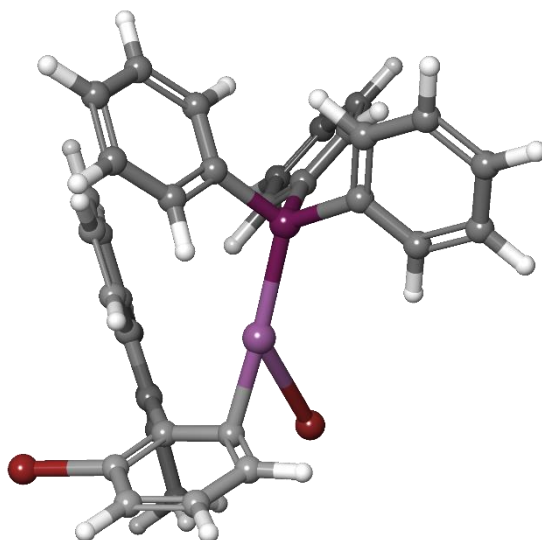


**Figure B24.** Modelling of Pd-complex of substrate **10** and ligand **3**.

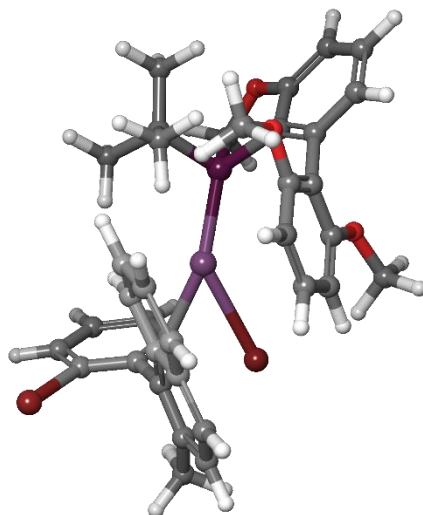


**Figure B25.** Modelling of Pd-complex of substrate **10** and ligand **4** with configuration (R,P).

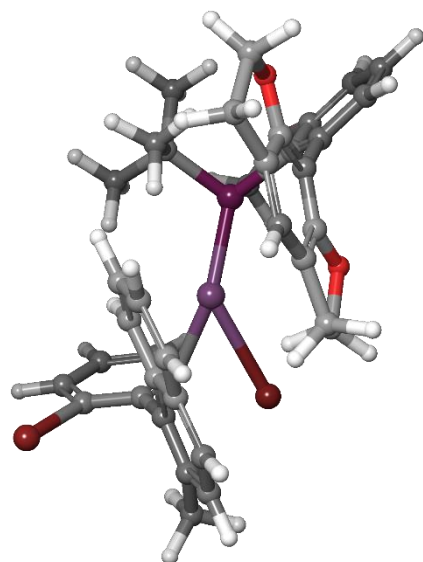


**Figure B26.** Modelling of Pd-complex of substrate **10** and ligand **5** with configuration (R,P).